Regioselectivities of the Insertion Reactions of Unsymmetrical Alkynes with the Nickelacycles [NiBr($C_6H_4CH_2PPh_2$-2)(L)] (L = Tertiary Phosphine)

Alison J. Edwards,[†,‡] Stuart A. Macgregor,[§] A. David Rae,[†,‡] Eric Wenger,*[,†] and Anthony C. Willis[†,‡]

Research School of Chemistry, Australian National University, Canberra, A.C.T. 0200, Australia, and Department of Chemistry, Heriot-Watt University, Riccarton, Edinburgh EH14 4AS, U.K.

Received February 12, 2001

The regioselectivities of the insertions of various alkynes into the Ni−Ph bond of the five-membered nickelacycles [NiBr($C_6H_4CH_2PPh_2$)(PR_3)] (PR_3 = PEt_3 (**2a**), $PPhBz_2$ (**2b**)) have been determined by multinuclear NMR spectroscopic studies of the products. In some cases, the resulting seven-membered nickelacycles have also been structurally characterized by X-ray analyses. The results show that electronic factors are very important in controlling the regioselectivity of these insertion reactions. For example, insertion of MeC≡CCO_2Me into **2b** forms mainly [NiBr{*o*-C(Me)=C(CO_2Me)$C_6H_4CH_2PPh_2$}($PPhBz_2$)] (**4b**), whereas CF_3C≡CCO_2Et gives exclusively the alternative regioisomer (**10b**). On the basis of these observations, a model based on frontier orbital interactions is proposed. The alkynylphosphines RC≡CPPh_2 insert regiospecifically into the Ni−C bonds of **2a**,**b** to give initially complexes that contain three-membered phosphanickelacycles formed by coordination of the PPh_2 group to the adjacent metal. These species are unstable and subsequently dimerize (R = CO_2Me) or undergo rearrangement (R = Me, Ph) to give a bicyclic nickelacycle in which the metal is part of both a six- and a four-membered ring.

Introduction

The insertions of alkynes and alkenes into metal−carbon bonds are very important reactions in organometallic chemistry and organic synthesis, and good regioselectivity or even complete regiocontrol in these reactions is essential. Complexes of group 10 metals are of particular importance in this context.[1−3] In particular, the reactions of nickelacycles and palladacycles give entries into synthetically important poly- or heterocyclic molecules.[4−14] Several mechanistic studies of the insertions of alkynes into Ni−C and Pd−C bonds have been reported.[15−20] Surprisingly, no detailed investigations into the factors governing the regioselectivity of these reactions have been published. Both electronic and steric arguments have been used to explain the substitution patterns of the products, but neither could be applied satisfactorily in all cases. For example, two investigations of the insertions of ^{t}BuC≡CMe into Ni−C and Pd−C bonds have concluded that these reactions were under steric control,[17,21] whereas the regioselectivities of the reactions of ester-activated alkynes with nickelaindenes are better accounted for by invoking electronic factors.[22] Our interest in the reactions of

* To whom correspondence should be addressed. E-mail: wenger@rsc.anu.edu.au.
† Australian National University.
‡ Single-Crystal X-ray Diffraction Unit.
§ Heriot-Watt University.

(1) Smith, A. K. In *Comprehensive Organometallic Chemistry II*; Abel, E. W., Stone, F. G. A., Wilkinson, G., Puddephatt, R. J., Eds.; Elsevier: Oxford, U.K., 1995; Vol. 9, p 29.
(2) Canty, A. J. In *Comprehensive Organometallic Chemistry II*; Abel, E. W., Stone, F. G. A, Wilkinson, G., Puddephatt, R. J., Eds.; Elsevier: Oxford, U.K., 1995; Vol. 9, p 225.
(3) Anderson, G. K. In *Comprehensive Organometallic Chemistry II*; Abel, E. W., Stone, F. G. A., Wilkinson, G., Puddephatt, R. J., Eds.; Elsevier: Oxford, U.K., 1995; Vol. 9, p 431.
(4) Jolly, P. W. In *Comprehensive Organometallic Chemistry*; Wilkinson, G., Stone, F. G. A., Abel, E. W., Eds.; Pergamon: Oxford, U.K., 1982; Vol. 8, p 649.
(5) Ryabov, A. D. *Synthesis* **1985**, 233.
(6) Lindner, E. *Adv. Heterocycl. Chem.* **1986**, *39*, 237.
(7) Bennett, M. A. *Pure Appl. Chem.* **1989**, *61*, 1695.
(8) Pfeffer, M. *Recl. Trav. Chim. Pays-Bas* **1990**, *109*, 567.
(9) Cámpora, J.; Paneque, M.; Poveda, M. L.; Carmona, E. *Synlett* **1994**, 465.
(10) Buchwald, S. L.; Broene, R. D. In *Comprehensive Organometallic Chemistry II*; Abel, E. W., Stone, F. G. A., Wilkinson, G., Hegedus, L. S., Eds.; Pergamon: Oxford, U.K., 1995; Vol. 12, p 771.
(11) Bennett, M. A.; Wenger, E. *Chem. Ber./Recl.* **1997**, *130*, 1029.
(12) Spencer, J.; Pfeffer, M. In *Advances in Metal-Organic Chemistry*; Liebeskind, L. S., Ed.; JAI: Stamford, CT, 1998; Vol. 6, p 104.
(13) Jones, W. M.; Klosin, J. *Adv. Organomet. Chem.* **1998**, *42*, 147.
(14) Cámpora, J.; Palma, P.; Carmona, E. *Coord. Chem. Rev.* **1999**, *193−195*, 207.
(15) Martinez, M.; Muller, G.; Panyella, D.; Rocamora, M.; Solans, X.; Font-Bardía, M. *Organometallics* **1995**, *14*, 5552.
(16) Samsel, E. G.; Norton, J. R. *J. Am. Chem. Soc.* **1984**, *106*, 5505.
(17) Huggins, J. M.; Bergman, R. G. *J. Am. Chem. Soc.* **1981**, *103*, 3002.
(18) de Vaal, P.; Dedieu, A. *J. Organomet. Chem.* **1994**, *478*, 121.
(19) Ryabov, A. D.; van Eldik, R.; Le Borgne, G.; Pfeffer, M. *Organometallics* **1993**, *12*, 1386.
(20) Ferstl, W.; Sakodinskaya, I. K.; Beydoun-Sutter, N.; Le Borgne, G.; Pfeffer, M.; Ryabov, A. D. *Organometallics* **1997**, *16*, 411.
(21) Spencer, J.; Pfeffer, M.; Kyritsakas, N.; Fischer, J. *Organometallics* **1995**, *14*, 2214.
(22) Bennett, M. A.; Wenger, E. *Organometallics* **1995**, *14*, 1267.

10.1021/om0101083 CCC: $20.00
Publication on Web 06/01/2001

Scheme 1

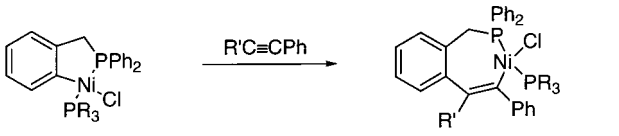

R' = Ph; PR_3 = PMe_2Ph, PEt_3, PBz_3
R' = CO_2Et; PR_3 = PBz_3 (**1**)

alkynes with five-membered nickelacycles started with the discovery that benzyne−nickel complexes can insert 2 equiv of alkynes to give substituted naphthalenes with various regiospecificities. For example, *tert*-butylacetylene leads to a 1,3-disubstituted species, whereas methyl 2-butynoate gives a symmetrical species with the carboxylate groups in the 2,3-positions.[22−24] These reactions are believed to take place via initial formation of a five-membered nickelacyclopentene complex. Subsequent insertion into either the Ni−vinyl or −aryl bond is assumed to yield a seven-membered species, which cannot be identified because of fast reductive elimination to the naphthalene product. Therefore, nickelacycles more suited to a systematic study of their reactions with alkynes were required.

Five-membered phosphanickelacycles [NiCl(*o*-C_6H_4-CH_2PPh_2)(PR_3)] (PR_3 = PMe_2Ph, PEt_3, PBz_3; Bz = benzyl, CH_2Ph) have been reported to react with alkynes, leading to stable seven-membered metallacycles by insertions into the Ni−aryl bond (Scheme 1).[25] One reaction with an unsymmetrical alkyne, PhC≡CCO_2Et, was carried out, leading to the product **1**, in which the phenyl substituent is located next to the metal; the structure of **1** was confirmed by X-ray analysis.

Therefore, we have chosen to carry out a systematic study of the insertion reactions of a large variety of alkynes using the analogous five-membered nickelacycles [NiBr($C_6H_4CH_2PPh_2$-2)(PR_3)] (PR_3 = PEt_3 (**2a**), $PPhBz_2$ (**2b**)), and the results are presented here. This investigation has been carried out primarily by use of multinuclear NMR spectroscopy to identify the different regioisomers. Several key products have been isolated and their structures confirmed by X-ray analyses. The observed regioselectivities will be discussed.

Experimental Results

The nickelacycles **2a** and **2b** were obtained as stable yellow solids after oxidative addition of *o*-$BrC_6H_4CH_2$-PPh_2 with [Ni(cod)$_2$] in the presence of 1 equiv of the corresponding tertiary phosphine, as described by Muller.[25] These complexes are planar and show only one signal for the benzylic CH_2 group of the metallacycle in the ^{1}H NMR spectrum. Treatment of these complexes with various unsymmetrical alkynes resulted in the formation of seven-membered nickelacycles, the geometries of which were determined spectroscopically. The results are summarized in Scheme 2. The metallacycles are nonplanar and show two complicated ^{1}H NMR signals for the inequivalent benzylic protons of the nickelacycle in the region δ_H 3.0−4.0. In the case of the reactions carried out with **2b**, four additional multiplets for the inequivalent benzylic protons of the auxiliary bis(benzyl)phenylphosphine ligand (PBz_2Ph) are also present in the same region. The triethylphosphine CH_2 groups for the products arising from **2a** are also inequivalent and form two A_3BCX multiplets in the region δ_H 1.60−1.80.

Scheme 2

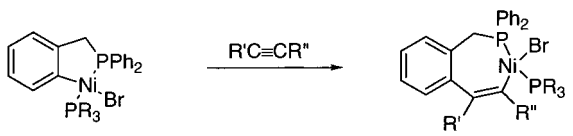

2a
2b

a: PR_3 = PEt_3
b: PR_3 = $PPhBz_2$

3a: R' = CO_2Et, R" = Ph

4a: R' = CO_2Me, R" = Me

4b: R' = CO_2Me, R" = Me (major)
5b: R' = Me, R" = CO_2Me

6a: R' = H, R" = CO_2Me
7a: R' = CO_2Me, R" = H (trace)

6b: R' = H, R" = CO_2Me (major)
7b: R' = CO_2Me, R" = H

8a: R' = H, R" = $CO_2{}^tBu$ (major)
9a: R' = $CO_2{}^tBu$, R" = H

10b: R' = CF_3, R" = CO_2Et

11a: R' = H, R" = ^{t}Bu

12a: R' = H, R" = Ph

12b: R' = H, R" = Ph

13a: R' = H, R" = $SiMe_3$

14b: R' = Et, R" = Ph (major)
15b: R' = Ph, R" = Et

The seven-membered nickelacycles resulting from the reactions of **2b** are generally more stable than their PEt_3 analogues, but even so, only products bearing carboxylate substituents could be isolated as solids. The more electron-rich products arising from insertions of alkyl- or aryl-substituted alkynes or bearing PEt_3 as the auxiliary ligand are very labile and decompose readily. Hence, multinuclear NMR spectroscopy proved to be the most convenient technique to investigate these reactions.

(a) Insertions of Ester-Activated Alkynes. To assess the validity of the NMR techniques we planned to use, the insertion of ethyl phenylpropynoate was carried out with the five-membered phosphanickelacycle [NiBr(*o*-$C_6H_4CH_2PPh_2$}(PEt_3)] (**2a**). The reaction was clean and formed only the product [NiBr{*o*-C(Ph)=$C(CO_2Me)C_6H_4CH_2PPh_2$}(PEt_3)] (**3a**), in which the phenyl group on the vinyl moiety is adjacent to the metal, as expected from the earlier study described above.[25]

(23) Bennett, M. A.; Wenger, E. *Organometallics* **1996**, *15*, 5536.
(24) Bennett, M. A.; Cobley, C. J.; Rae, A. D.; Wenger, E.; Willis, A. C. *Organometallics* **2000**, *19*, 1522.
(25) Muller, G.; Panyella, D.; Rocamora, M.; Sales, J.; Font-Bardia, M.; Solans, X. *J. Chem. Soc., Dalton Trans.* **1993**, 2959.

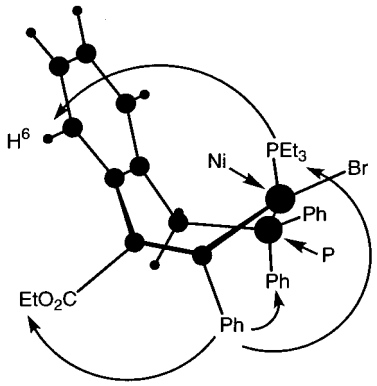

Figure 1. Principal magnetization transfers observed during the GOESY experiments with **3a**.

The ^{31}P NMR spectrum consists of two doublets, one at δ_P 6.9 for the PEt_3 ligand and one at δ_P 27.5 for the PPh_2 group, with a coupling constant of 301.7 Hz that is characteristic of a trans ^2J(PP) coupling. The 20 ppm upfield shift observed for the cyclometalated PPh_2 group, when compared to that of **2a** (δ_P 44.5), is characteristic of an increase of the metallacycle from five- to seven-membered as a result of the insertion of the alkyne into the Ni−C bond.[26] The regioselectivity of the insertion can be deduced from the ^{13}C NMR data of the product, especially those of the carbon atoms of the vinyl group resulting from the insertion of the alkyne. The marked deshielding of the α-vinyl carbon that is bonded to nickel (δ_C 173.91) can best be explained by delocalization of the double bond on to an ester group in the β position. Furthermore, the larger C−P coupling constants observed for the quaternary carbon of the phenyl substituent (13 and 6.6 Hz) when compared with those of the carboxylate group (5.2 and 2.5 Hz) are a good indication that the former is closer to the phosphine ligands and, hence, to the metal. The structure assigned to **3a** could be confirmed by use of the GOESY pulse sequence, which clearly showed that the PEt_3 ligand is in close contact with the phenyl group. Irradiation of the CH_2 group of PEt_3 (δ_H 1.50−1.75) shows magnetization transfer to the adjacent CH_3 groups (δ_H 0.70) and to the *ortho* protons of the phenyl substituents at δ_H 7.63. Some transfer is also observed to the proton H^6 (δ_H 7.87) (Figure 1), due to the boat-shaped conformation of the seven-membered ring as shown for structurally characterized examples below. These NMR experiments have been successful in assigning the structure of **3a**; hence, they have been applied to determine the geometries of the insertion products for all the alkynes discussed below.

The reaction of methyl 2-butynoate with **2a** is regiospecific and occurs in the same sense as that discussed above, hence the insertion product is formulated as [NiBr{*o*-C(Me)=C(CO_2Me)$C_6H_4CH_2PPh_2$}(PEt_3)] (**4a**). The ^{13}C NMR spectrum of **4a** shows a coupling of 7.6 Hz between one of the phosphorus atoms and the carbon of the vinylic methyl group, characteristic of a ^3J(CP) coupling, and the quaternary carbon bonded to nickel is even more deshielded than in **3a** (δ_C 197.00). GOESY experiments confirm that the methyl substituent in **4a** is indeed close to the PEt_3 ligand, as shown by the very clean magnetization transfer to the methyl substituent when the CH_3 group of PEt_3 (δ_H 1.03) is irradiated.

Reaction of methyl 2-butynoate with the analogous complex **2b**, bearing the more bulky tertiary phosphine PBz_2Ph, gives predominantly the same regioisomer (**4b**), but minor amounts of a second product (**5b**) are also observed. The ratio of **4b**/**5b** is solvent-dependent and varies from 7:1 for a reaction carried out in thf/C_6D_6 to 3.2:1 in CD_2Cl_2. The NMR data for **4b** are similar to those of **4a**, and in this case, the structure assigned to this compound from the NMR data was confirmed by X-ray analysis (see below). The minor compound (**5b**) has similar ^{31}P NMR data but shows a ^2J(PP) value for the coupling between the trans phosphine ligands ca. 50 Hz larger than that in **4b** (334 and 282 Hz, respectively). These data are comparable with those for the main insertion product obtained with HC≡CCO_2Me (see below); hence, **5b** is assumed to be the second insertion isomer in which the carboxylate is adjacent to nickel, viz. [NiBr{*o*-C(CO_2Me)=C(Me)$C_6H_4CH_2PPh_2$}($PPhBz_2$)].

In the case of HC≡CCO_2Me, the insertion reactions with both **2a** and **2b** give the two possible regioisomers, but the more abundant products always have the larger ^2J(PP) values. The reaction of methyl propynoate with **2a** is almost regiospecific, while the reaction with **2b** gives a 9:1 ratio of the two regioisomers. The ^{13}C NMR spectra of the main insertion products (**6a** and **6b**, respectively) show the vinyl carbon atoms bonded to nickel, easily identified by their characteristic two-bond coupling constants with the phosphorus atoms of ca. 39 and 30 Hz, at δ_C 149.05 and 149.25, these carbon atoms being much more shielded than those of **3a**, **4a**, or **4b**. These α-carbon atoms are quaternary, as shown by APT experiments; hence, they bear the carboxylate groups. The two vinylic CH carbon atoms are also readily located at ca. δ_C 142 with ^3J(CP) values of 6.3 and 5.8 Hz, respectively. The proximity of the ester groups to the auxiliary phosphine ligands was also confirmed by GOESY experiments. Therefore, the major isomers in this series of reactions can be formulated as [NiBr{*o*-C(CO_2Me)=C(H)$C_6H_4CH_2PPh_2$}(PR_3)] (PR_3 = PEt_3 (**6a**), $PPhBz_2$ (**6b**)) (Scheme 2), and the structure of **6b** has been confirmed by X-ray structure analysis (see below). The minor products are likely to be the alternative regioisomers [NiBr{*o*-C(H)=C(CO_2Me)$C_6H_4CH_2PPh_2$}-($PPhBz_2$)] (PR_3 = PEt_3 (**7a**), $PPhBz_2$ (**7b**)).

Similar reaction of HC≡$CCO_2{}^t$Bu with **2a** gives a mixture of products with NMR data almost identical with those of **6a** and **7a**. The main difference between this reaction and the regiospecific one of HC≡CCO_2Me is the increased proportion of the isomer having the vinylic carboxylate in the β-position (**9a**); thus, the ratio between [NiBr{*o*-C($CO_2{}^t$Bu)=C(H)$C_6H_4CH_2PPh_2$}(PEt_3)] (**8a**) and [NiBr{*o*-C(H)=C($CO_2{}^t$Bu)$C_6H_4CH_2PPh_2$}(PEt_3)] (**9a**) is 5:1, as measured by ^{31}P NMR spectroscopy.

The insertion reaction of CF_3C≡CCO_2Et with **2b** gives only one regioisomer. The ^{31}P NMR spectrum shows two doublets of quartets at δ_P 9.2 for PBz_2Ph and δ_P 32.2 for PPh_2 with a large value of ^2J(PP) (318.6 Hz) but a rather small P−F coupling constant between the respective phosphorus atoms and the CF_3 group (4.7 and

(26) Garrou, P. E. *Chem. Rev.* **1981**, *81*, 229.

5.2 Hz). The ^{13}C NMR resonance of the quaternary carbon atom adjacent to nickel also shows a small coupling with the fluorine atoms of CF_3 (2.5 Hz). This value is characteristic of a three-bond C−F coupling;[27,28] hence, this carbon does not bear the CF_3 group. Therefore, the proposed structure for this product is [NiBr{*o*-C(CO_2Et)=C(CF_3)$C_6H_4CH_2PPh_2$}(PPhBz$_2$)] (**10b**). Crystallization led to partial decomposition, and crystals of only mediocre quality were obtained, but the geometry of **10b** could nevertheless be confirmed by X-ray diffraction analysis.

(b) Insertions of Alkyl- or Aryl-Substituted Alkynes. The reactions of **2a** and **2b** with alkyl- and aryl-substituted alkynes were carried out exclusively in situ, as the resulting seven-membered nickelacycles decompose readily in solution. The insertion of HC≡C^{t}Bu into the Ni−C bond of **2a** gave only one regioisomer, having doublets in the ^{31}P NMR spectrum at δ_P 0.7 and 19.8. These signals are more shielded than those of the insertion products described above, but surprisingly the vinylic α-carbon is highly deshielded and its ^{13}C NMR signal is found at δ_C 173.88. This carbon is quaternary, which allows the insertion product to be tentatively formulated as [NiBr{*o*-C(^{t}Bu)=C(H)-$C_6H_4CH_2PPh_2$}(PEt$_3$)] (**11a**) (Scheme 2). A similar reaction carried out with HC≡CSiMe$_3$ led mainly to decomposition, but traces of an insertion compound (**13a**) could be observed by ^{31}P NMR spectroscopy. The data, especially the ^2J(PP) value, are similar to those of **11a**; hence, **13a** is believed to be an insertion product having the same geometry as **11a**.

Reaction of HC≡CPh with **2a** gave only one major insertion product (**12a**) that decomposed readily. The product of the analogous reaction carried out with **2b** was slightly less labile, and its ^{13}C NMR spectrum could be recorded. The main feature of the spectrum of this product (**12b**) is a resonance located at δ_C 160.40, which belongs to a quaternary vinylic α-carbon atom. As the ^{31}P NMR data for **12a** and **12b** are very similar, the structure proposed for the products of both insertions is [NiBr{*o*-C(Ph)=C(H)$C_6H_4CH_2PPh_2$}(PR$_3$)] (PR$_3$ = PEt$_3$ (**12a**), PBz$_2$Ph (**12b**)).

The insertion reaction of EtC≡CPh with **2b** gave a 11:1 mixture of two labile regioisomers. The phosphorus atoms of the major isomer (**14b**) are more shielded and have a ^2J(PP) value larger than those of the minor isomer (**15b**). The ^{13}C NMR signal for the quaternary α-carbon of **14b** is found at δ_C 148.75, but it is not possible to tell whether it bears the phenyl or the ethyl group. Investigation of **14b** by GOESY NMR experiments shows a large number of magnetization transfers, which suggest that this complex is very crowded. For example, irradiation of the signal at δ_H 2.87 corresponding to a benzylic proton of the PBz$_2$Ph ligand shows magnetization transfer to several protons (aromatic and benzylic) in the phosphine ligand, but also to the two ortho protons of the vinylic phenyl group (δ_H 6.92). This group is also in close contact with the axial phenyl ring of the cyclometalated PPh_2 group, as demonstrated by the irradiation of the ortho hydrogens of the latter group at δ_H 8.16 (see Experimental Section). These NMR experiments allow the unambiguous characterization of **14b** as being [NiBr{*o*-C(Ph)=C(Et)$C_6H_4CH_2PPh_2$}-(PPhBz$_2$)], the minor product **15b** being tentatively assigned to the alternative regioisomer [NiBr{*o*-C(Et)=C(Ph)$C_6H_4CH_2PPh_2$}(PPhBz$_2$)].

Scheme 3

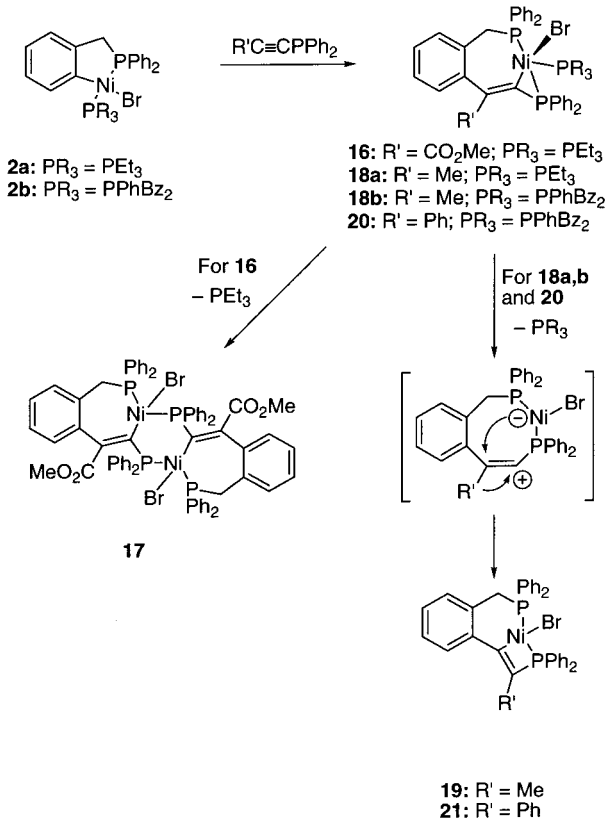

(c) Insertions of Alkynylphosphines. The results of these experiments are summarized in Scheme 3. Reaction of MeO$_2$CC≡CPPh$_2$ with **2a** gave one major insertion product (>90% by ^{31}P NMR spectroscopy) having three sets of ^{31}P NMR signals: two doublets of doublets at δ_P 13.8 and 28.6 due to PEt$_3$ and the cyclometalated PPh_2 groups, respectively, and a doublet of doublets at δ_P −101.5. The latter phosphine is trans to the CH_2PPh_2 group, as shown by the ^2J(PP) value of 239 Hz. This very shielded signal can be assigned to a three-membered phosphanickelacycle with the carbon atom being sp^2-hybridized. Five-coordinate nickel complexes possessing such fragments have recently been obtained by protonation of η^2-coordinated alkynylphosphines,[29] and their ^{31}P NMR spectra show similarly shielded signals. An insertion product with such a geometry can only be formed if the PPh_2 group of the incoming alkynylphosphine is located next to the metal. The presence of the carboxylate group on the β-carbon atom of the vinyl group, with respect to the nickel, is also suggested by the strongly deshielded quaternary carbon atom bonded to the metal (multiplet at δ_C

(27) Bégué, J.-P.; Bonnet-Delpon, D.; Mesureur, D.; Ourévitch, M. *Magn. Reson. Chem.* **1991**, *29*, 675.

(28) Matsubara, K.; Oba, A.; Usui, Y. *Magn. Reson. Chem.* **1998**, *36*, 761.

(29) Bennett, M. A.; Castro, J.; Edwards, A. J.; Kopp, M. R.; Wenger, E.; Willis, A. C. *Organometallics* **2001**, *20*, 980.

170.00−171.10). Therefore, the structure proposed for this product is the five-coordinated nickelacycle [NiBr{*o*-C(PPh$_2$)=C(CO$_2$Me)C$_6$H$_4$CH$_2$PPh$_2$}(PEt$_3$)] (**16**) (Scheme 3). Over time, complex **16** loses PEt$_3$ to give the dimeric species [NiBr{μ-*o*-C(PPh$_2$)=C(CO$_2$Me)C$_6$H$_4$CH$_2$PPh$_2$}]$_2$ (**17**). The latter complex has been identified by X-ray analysis, confirming the assignment of the vinylic substituents of the unstable species **16** (see below).

Treatment of **2a** or **2b** with MeC≡CPPh$_2$ very slowly forms species similar to **16**, viz. [NiBr{*o*-C(PPh$_2$)=C(Me)C$_6$H$_4$CH$_2$PPh$_2$}(PR$_3$)] (PR$_3$ = PEt$_3$ (**18a**), PBz$_2$Ph (**18b**)), with the characteristic ^{31}P NMR signals of the three-membered nickelacycles at δ_P −112.9 and −106.8, respectively. However, the products are unstable; the former decomposes readily, while the latter rearranges with loss of PBz$_2$Ph to give a new species having a ^{31}P NMR signal at δ_P −71.0 (**19**). The latter chemical shift is indicative of a four-membered nickelacycle,[26] but further identification proved impossible due to decomposition of the reaction mixture.

Similar reaction of **2b** with PhC≡CPPh$_2$ gives very broad ^{31}P NMR signals. After 48 h at 30 °C, the complicated spectrum shows the mixture to contain [NiBr{*o*-C(PPh$_2$)=C(Ph)C$_6$H$_4$CH$_2$PPh$_2$}(PPhBz$_2$)] (**20**) (doublet at δ_P −101.0), a second species with a doublet at δ_P −68.0 (**21**), and free PBz$_2$Ph. The latter complex, however, is more stable than its analogue **19** and could be purified by passing the solution through a silica gel column. Crystallization gave single crystals that were suitable for X-ray analysis, and complex **21** could be identified as being the bicyclic complex [NiBr{*o*-(PPh$_2$)(Ph)C=CC$_6$H$_4$CH$_2$PPh$_2$}] (see below). This compound contains a four-membered phosphanickelacycle, hence the chemical shift at δ_P −68.0, whose formation can be explained by elimination of PBz$_2$Ph and cleavage of the Ni−C bond, followed by a 1,2-shift of the phenyl substituent to the positively charged α-carbon atom of the resulting zwitterionic intermediate (Scheme 3). By analogy, the unstable compound **19** derived from MeC≡CPPh$_2$ is tentatively assigned as [NiBr{*o*-(PPh$_2$)(Me)C=CC$_6$H$_4$CH$_2$PPh$_2$}]. As the formation of these rearrangement products was beyond the scope of the present work, these reactions were not studied further.

(d) Molecular Structures of [NiBr{*o*-C(Me)=C(CO$_2$Me)C$_6$H$_4$CH$_2$PPh$_2$}(PPhBz$_2$)] (4b), [NiBr{*o*-C(CO$_2$Me)=C(H)C$_6$H$_4$CH$_2$PPh$_2$}(PPhBz$_2$)] (6b), [NiBr{*o*-C(CO$_2$Me)=C(CF$_3$)C$_6$H$_4$CH$_2$PPh$_2$}(PPhBz$_2$)] (10b), [NiBr{μ-*o*-C(PPh$_2$)=C(CO$_2$Me)C$_6$H$_4$CH$_2$PPh$_2$}]$_2$ (17), and [NiBr{*o*-(PPh$_2$)(Ph)C=CC$_6$H$_4$CH$_2$PPh$_2$}] (21). The molecular geometries of **4b**, **6b**, **10b**, **17**, and **21** are shown, together with the atom labelings, in Figures 2−6, respectively; corresponding selected interatomic distances and angles are listed in Tables 1−5.

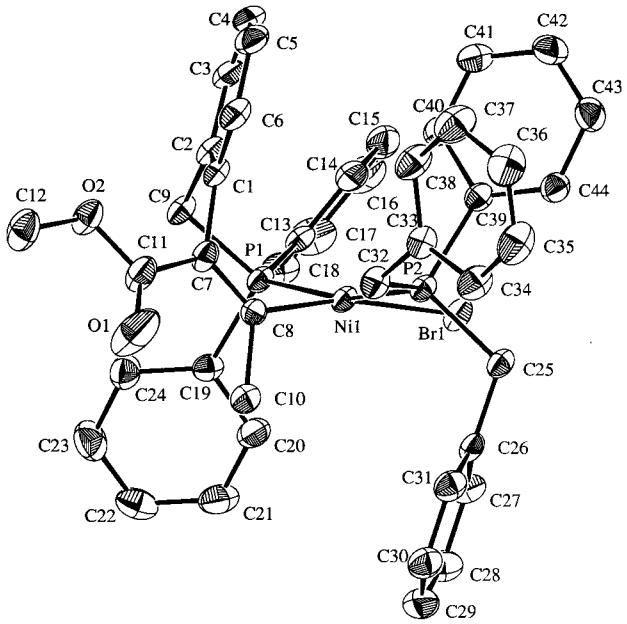

Figure 2. Molecular structure of **4b** with selected atom labeling. Thermal ellipsoids show 30% probability levels; hydrogen atoms have been omitted for clarity.

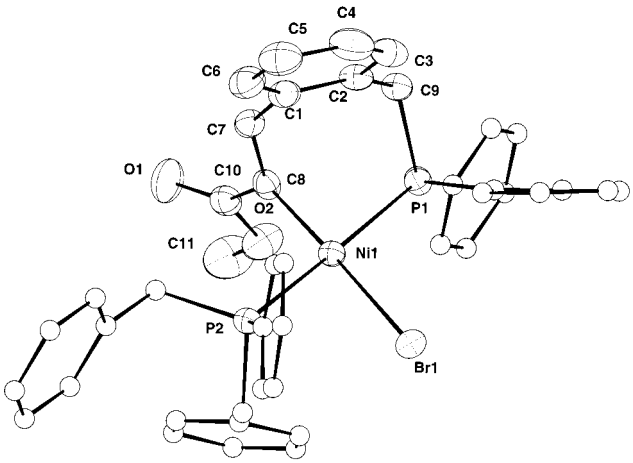

Figure 3. Molecular structure of **6b** with selected atom labeling. Thermal ellipsoids show 50% probability levels; hydrogen atoms have been omitted for clarity, and carbon atoms of the PBz$_2$Ph and PPh$_2$ groups have been drawn as circles with small radii.

The nickel atom in complex **4b** is in a distorted-square-planar environment, with atom C(8) being 0.8 Å from the best-fit plane defined by Ni−Br−P(1)−P(2). The seven-membered ring is in a boat-shaped configuration, with the plane of the aromatic ring C(1)−C(6) being at right angles (95°) to the coordination plane of the nickel. This geometry renders the two phenyl rings of the cyclometalated PPh$_2$ group and the two benzyl groups of the auxiliary phosphine separately inequivalent. This is in agreement with the four inequivalent benzylic protons present in the ^{1}H NMR spectrum of **4b** and with the GOESY experiments which show close contact between the aromatic proton bonded to C(6) and the auxiliary phosphine ligand. Similar geometries have been observed for other seven-membered nickelacycles

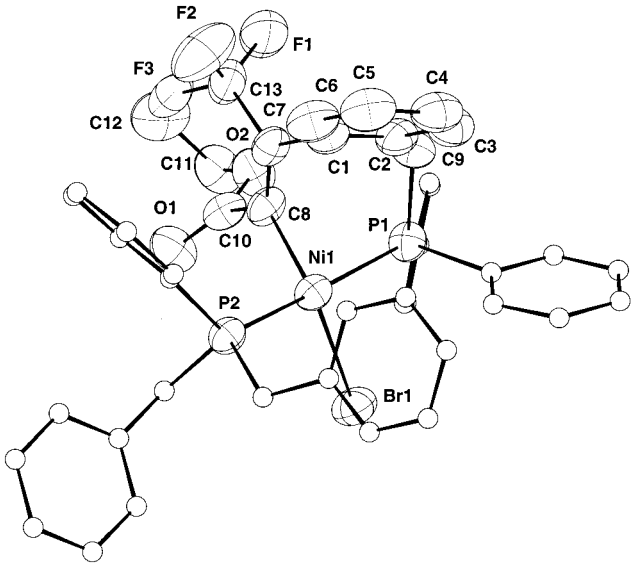

Figure 4. Molecular structure of **10b** with selected atom labeling. Thermal ellipsoids show 50% probability levels; hydrogen atoms have been omitted for clarity, and carbon atoms of the PBz_2Ph and PPh_2 groups have been drawn as circles with small radii.

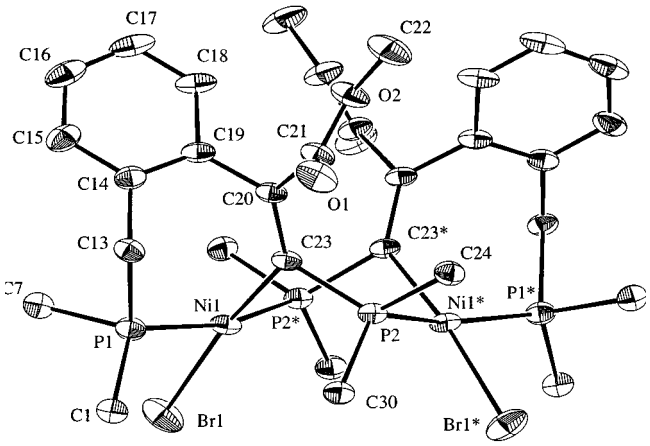

Figure 5. Molecular structure of **17** with selected atom labeling. Asterisks indicate atoms generated by the crystallographic 2-fold summetry. Thermal ellipsoids show 30% probability levels; phenyl carbon atoms of the PPh_2 groups, except those directly attached to phosphorus (C(1), C(7), C(24) and C(30)), and all hydrogen atoms have been omitted for clarity.

such as complex **1**,[25] [NiBr{C(CO_2Me)=C(CO_2Me)$C_{10}H_6$-CF_2CF_2}(dcpe)] (**22**), produced by insertion of DMAD into the Ni−naphthyl bond of [Ni(3-$C_{10}H_6CF_2CF_2$-2}-(dcpe)],[30] and the carboxylato complex resulting from insertion of CO_2 into the Ni−phenyl bond of the nickelacycle [Ni(*o*-$C_6H_4CMe_2CH_2$}(PMe_3)$_2$].[31,32] The Ni−C(8) distance (1.88 Å) is similar to those of other Ni−vinyl bonds in such systems (1.92 Å in **22** or 1.90 Å in **1**). The distance C(7)−C(8) (1.35 Å) is typical of a C=C bond,

(30) Bennett, M. A.; Hockless, D. C. R.; Wenger, E. *Organometallics* **1995**, *14*, 2091.

(31) Carmona, E.; Palma, P.; Paneque, M.; Poveda, M. L.; Gutiérrez-Puebla, E.; Monge, A. *J. Am. Chem. Soc.* **1986**, *108*, 6424.

(32) Carmona, E.; Gutiérrez-Puebla, E.; Marín, J. M.; Monge, A.; Paneque, M.; Poveda, M. L.; Ruiz, C. *J. Am. Chem. Soc.* **1989**, *111*, 2883.

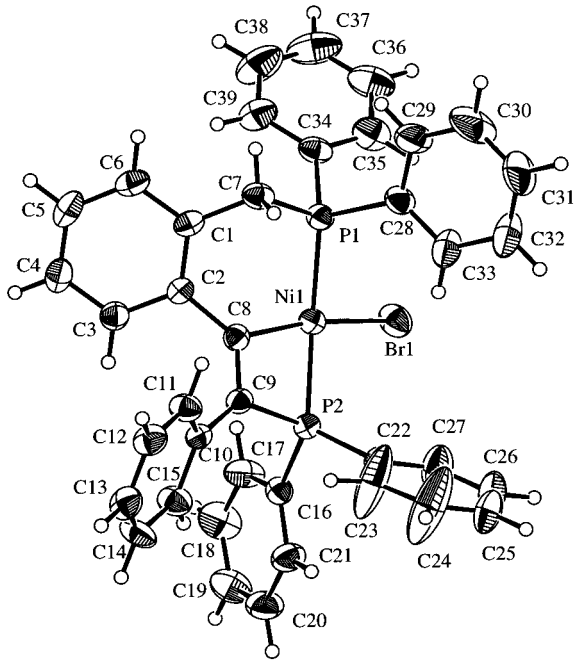

Figure 6. Molecular structure of **21** with selected atom labeling. Thermal ellipsoids show 30% probability levels; hydrogen atoms have been drawn as circles with small radii.

Table 1. Selected Bond Lengths (Å) and Bond Angles (deg) for 4b

Ni(1)−Br(1)	2.3670(6)	Ni(1)−P(1)	2.1834(9)
Ni(1)−P(2)	2.2300(9)	Ni(1)−C(8)	1.880(3)
C(7)−C(8)	1.349(5)	C(8)−C(10)	1.507(4)
P(1)−Ni(1)−P(2)	165.65(4)	Br(1)−Ni(1)−P(1)	95.59(3)
Ni(1)−C(8)−C(7)	128.1(2)	Ni(1)−P(1)−C(9)	112.6(1)
C(7)−C(8)−C(10)	124.8(3)	P(2)−Ni(1)−C(8)	91.2(1)

Table 2. Selected Bond Lengths (Å) and Bond Angles (deg) for 6b

Ni(1)−Br(1)	2.3544(3)	Ni(1)−P(1)	2.1799(5)
Ni(1)−P(2)	2.2167(5)	Ni(1)−C(8)	1.9049(18)
C(7)−C(8)	1.337(3)	C(8)−C(10)	1.495(3)
P(1)−Ni(1)−P(2)	167.979(19)	Br(1)−Ni(1)−P(1)	91.017(14)
Ni(1)−C(8)−C(7)	128.79(14)	Ni(1)−P(1)−C(9)	114.94(6)
C(7)−C(8)−C(10)	114.16(16)	P(2)−Ni(1)−C(8)	92.08(5)

Table 3. Selected Bond Lengths (Å) and Bond Angles (deg) for 10b

Ni(1)−Br(1)	2.3505(15)	Ni(1)−P(1)	2.201(3)
Ni(1)−P(2)	2.246(3)	Ni(1)−C(8)	1.870(9)
C(7)−C(8)	1.340(13)	C(8)−C(10)	1.483(14)
C(7)−C(13)	1.512(14)		
P(1)−Ni(1)−P(2)	166.64(11)	Br(1)−Ni(1)−P(1)	93.82(8)
Ni(1)−C(8)−C(7)	132.1(7)	Ni(1)−P(1)−C(9)	112.3(4)
C(7)−C(8)−C(10)	121.0(8)	P(2)−Ni(1)−C(8)	91.2(3)

and its substitution pattern is identical with that predicted by multinuclear spectroscopy: viz., the methyl C(10) bonded to C(8) and the carboxylate carbon C(11) bonded to C(7).

The structure of complex **6b** is similar to that described above and differs mainly in the position occupied by the carboxylate, which is now bonded to C(8). The nickel atom is in a distorted-square-planar environment, with atoms C(8) and P(1) being −0.16 and 0.45 Å, respectively, from the plane defined by Ni−Br−P(2). The plane of the aromatic ring C(1)−C(6) has a dihedral angle of 84° with the coordination plane of the nickel.

Table 4. Selected Bond Lengths (Å) and Bond Angles (deg) for 17

Ni(1)−P(1)	2.232(5)	Ni(1)−P(2*)	2.238(5)
Ni(1)−Br(1)	2.350(4)	Ni(1)−C(23)	1.934(18)
C(20)−C(23)	1.354(23)	P(2)−C(23)	1.796(18)
P(1)−Ni(1)−P(2*)	172.4(6)	Br(1)−Ni(1)−P(1)	88.9(2)
Br(1)−Ni(1)−P(2*)	89.1(2)	Br(1)−Ni(1)−C(23)	172.4(6)
Ni(1)−C(23)−P(2)	101.7(8)	Ni(1)−C(23)−C(20)	130.6(15)
C(19)−C(20)−C(23)	124.0(17)	Ni(1*)−P(2)−C(23)	116.7(6)

Table 5. Selected Bond Lengths (Å) and Bond Angles (deg) for 21

Ni(1)−P(1)	2.186(2)	Ni(1)−P(2)	2.175(2)
Ni(1)−C(8)	1.923(7)	Ni(1)−Br(1)	2.356(2)
C(2)−C(8)	1.475(9)	C(8)−C(9)	1.355(9)
C(9)−P(2)	1.799(7)	C(7)−P(1)	1.836(8)
P(1)−Ni(1)−P(2)	150.4(1)	Br(1)−Ni(1)−C(8)	168.0(2)
P(1)−Ni(1)−C(8)	92.7(2)	C(8)−Ni(1)−P(2)	70.1(2)
Ni(1)−C(8)−C(9)	108.6(6)	C(8)−C(9)−P(2)	96.0(5)
C(8)−C(9)−C(10)	130.8(7)	Ni(1)−P(2)−C(9)	84.4(3)
Ni(1)−C(8)−C(2)	124.1(5)	Ni(1)−P(1)−C(7)	111.7(3)

The molecular structure of **10b** is of poorer quality but shows clearly that the carboxylate group is attached to C(8), whereas the CF_3 group is bonded to C(7). The nickel atom is in a slightly more distorted square planar environment than that of **6b**, the atoms C(8) and P(1) being −0.55 and 0.55 Å, respectively, from the plane defined by Ni−Br−P(2). The boat-shaped conformation is similar to that of **4b** and **6b**, as shown by the dihedral angle of 96° between the plane of the aromatic ring C(1)−C(6) and the coordination plane of the nickel.

The molecular structure of the dimeric complex **17** shows a distorted-square-planar arrangement around the nickel. Each metal is part of a bicyclic system. The first cycle is the seven-membered ring resulting from insertion of the alkynylphosphine $MeO_2CC{\equiv}CPPh_2$ into the Ni−C bond of **2a**, in which the PPh_2 group is adjacent to nickel. The second cycle is a boat-shaped six-membered ring connecting two nickelacycle units via coordination of the PPh_2 group of one metallacycle, located on the vinyl carbons C(23) or C(23*), to the nickel atom of the second one. The Ni−C distance (1.93 Å) is slightly longer than the ones in **4b**, **6b**, and **10b**, but all the other distances are unexceptional.

In the bicyclic complex **21**, the coordination geometry around the nickel is quite distorted from planarity, due to the steric constraints imposed by the metal atom's being part of both a four- and a six-membered ring. The four-membered nickelacycle Ni−P(2)−C(8)−C(9) is planar, but the phosphorus atom P(1) lies 0.85 Å above this plane, while the bromine atom lies 0.17 Å below the plane. The Ni−C(8) bond length (1.92 Å) is similar to the values discussed above, while the Ni−P(2) distance is in the normal range for a Ni−P bond. The double bond between C(8) and C(9) is only slightly elongated (1.36 Å) when compared to a standard C=C bond and, as a result, none of the angles in the four-membered ring is close to 90°. The carbon atom C(9) is substituted by both a phenyl group and a PPh_2 group. The six-membered nickelacycle has a strained boat-shaped conformation, but all the bond lengths are in the usual ranges.

Discussion

Five-membered nickelacycles proved to be very useful for the study of the insertions of unsymmetrical alkynes.

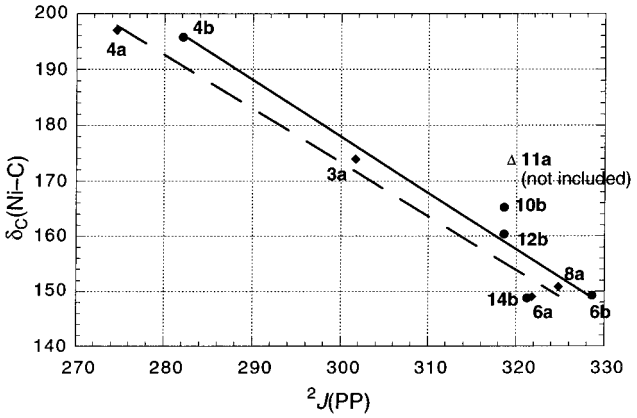

Figure 7. Graph of $\delta(C^\alpha)$ vs ^2J(PP) for seven-membered nickelacycles [NiBr{*o*-$C^\alpha(R^1){=}C(R^2)C_6H_4CH_2PPh_2$}(L)]. The linear regressions gave $y = -1.019x + 483.6$ for L = PEt_3 (complex **11a** excluded) and $y = -0.970x + 464.3$ for L = PBz_2Ph.

Table 6. ^{13}C NMR Chemical Shifts (ppm) of Ni−C^α and Trans ^2J(PP) Values (Hz) for Seven-Membered Nickelacycles.

		Ni−$C^\alpha(R^1){=}C^\beta(R^2)$			
entry	complex	R^1	R^2	$\delta_C(C^\alpha)$	$^2J_{PP}$
1	**3a**	Ph	CO_2Et	173.91	301.7
2	**4a**	Me	CO_2Me	197.00	274.6
3	**6a**	CO_2Me	H	149.05	321.8
4	**8a**	$CO_2{}^tBu$	H	150.80	324.8
5	**11a**	tBu	H	173.88	319.4
6	**4b**	Me	CO_2Me	195.77	282.1
7	**10b**	CO_2Et	CF_3	165.24	318.6
8	**6b**	CO_2Me	H	149.25	328.6
9	**12b**	Ph	H	160.40	318.6
10	**14b**	Ph	Et	148.75	321.2

The clean regioselectivities and the relative stabilities of the resulting seven-membered metallacycles in solution allowed the products to be identified by the use of multinuclear NMR techniques, even though they often could not be isolated. The magnetization transfers observed during the GOESY experiments enable the substitution patterns of the insertion products to be determined, and the ^{13}C NMR data of the vinylic carbon atoms bonded to nickel give invaluable information about the attached groups and about the electron density of the vinyl moiety. For example, when an electron-withdrawing substituent is located in the β-position with respect to the nickel atom, the α-carbon is highly deshielded (see Table 6, entries 1, 2, and 6). The only exception is complex **11a** (entry 5), in which C^α is very deshielded even though this carbon is substituted with a *tert*-butyl group and no electron-withdrawing group is present. Possibly, this low-field chemical shift arises from a distortion of the sp^2 geometry of the α-carbon caused by the steric interaction of the substituent with the auxiliary PEt_3 ligand.

Analysis of the NMR data also showed that a linear correlation exists between the ^{13}C NMR chemical shift of C^α, i.e., its electron density, and the corresponding ^2J(PP) value in the complex, as illustrated in Figure 7; the more electron-deficient the α-carbon, the smaller the coupling constant. The reasons for the influence of a vinylic cis substituent on a trans coupling between two phosphine groups are unclear. The lines obtained for

the PEt_3 and PBz_2Ph complexes are almost parallel, with a horizontal shift of ca. 10 Hz between the two slopes.

The regioselectivities for the alkyne insertions into the Ni−C bonds of **2a** and **2b** are only slightly affected by changing the auxiliary ligands from PEt_3 to PBz_2Ph and are determined primarily by the nature of the alkyne substituents.

The insertions of *tert*-butylacetylene, phenylacetylene, and 1-phenyl-1-butyne formed unstable nickelacycles having the *tert*-butyl or phenyl groups adjacent to nickel. Such regioselectivities have precedents. These alkynes have been shown to insert similarly into Ni−Me bonds, and the proposed mechanism involves attack of the methyl group onto the less-hindered carbon atom of the alkyne.[17,33]

The regioselectivity determined in solution for the insertion of ethyl phenylpropynoate with **2a** is in agreement with the solid-state structure of the product reported for the analogous reaction with [NiCl(*o*-C_6H_4-CH_2PPh_2)(PBz_3)]:[25] i.e., the phenyl group is adjacent to the metal. In the case of the reactions of methyl 2-butynoate with **2a** and **2b**, the same substitution pattern is preferred, as shown by both NMR techniques and X-ray crystallography; replacement of the phenyl group by a methyl group does not alter the regiochemistry of the reaction. Similar regioselectivities have been observed with related benzyldimethylamine and benzylthioether cyclopalladated dimers [PdCl{*o*-$C_6H_4CH_2$-X)]$_2$) (X = NMe_2, SR),[34−37] but unfortunately, direct comparison with phosphapalladacycles is not possible, as the latter have been shown to be inert toward insertions of alkynes under normal conditions.[38] To explain the regiochemistry observed for the reactions of ethyl phenylpropynoate with these palladacycles, possible hydrogen bonding between the carboxylate and proton H^6 of the metallacyclic phenyl group before insertion into the Pd−C bond has been suggested.

The reactions of both methyl and *tert*-butyl propynoates with **2a** and **2b** give preferentially the opposite regioisomer; i.e., the major products bear the carboxylate groups adjacent to the metal and its bulky auxiliary phosphine ligand, clearly a manifestation of electronic control. However, as a minor effect, the steric interaction between those two groups can influence the ratio between the isomers. The reaction of methyl propynoate with **2a**, having PEt_3 as auxiliary ligand, gives almost regiospecifically **6a**, whereas the same reaction carried out with the PBz_2Ph analogue **2b** forms some of the isomer having the carboxylate group adjacent to phenyl (**7b**). Also, when the size of the ester group is increased, e.g. by use of *tert*-butyl propynoate, the amount of the second isomer increases correspondingly. The fact that these insertion reactions are sensitive to both the size of the carboxylate group and the size of the auxiliary phosphine ligand is a good indication that both are present in the coordination sphere of the metal during the transition state, hence suggesting that the reaction proceeds via a five-coordinate associative mechanism. This observation is in agreement with kinetic studies carried out with analogous phosphanickelacycles.[15]

Scheme 4

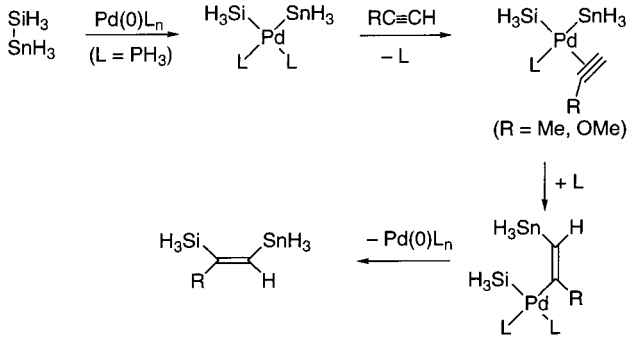

The reaction of **2b** with ethyl perfluoro-2-butynoate gives exclusively the regioisomer in which the carboxylate group is adjacent to the metal (**10b**). This is a complete reversal of regioselectivity in comparison to the insertions of the analogous nonfluorinated alkyne leading to **4a** and **4b**. This observation again suggests that electronic factors contribute greatly to the regiochemistry of alkyne insertions.

One example of a possible electronic control has been reported for the regioselective silastannation of alkynes such as propyne and methoxyacetylene, catalyzed by a palladium complex.[39] This theoretical study showed that the reaction takes place via insertion of the alkyne into a Pd−Sn bond (Scheme 4) and that the main interaction responsible for the reactivity is electron donation from the HOMO of the palladium moiety (predominantly the Pd d orbital in bonding combination with a Sn p orbital). On the other hand, the regiochemistry, i.e., the orientation of the alkyne, is mainly dictated by an interaction of the alkyne HOMO, polarized by the substituent, with the LUMO of the palladium fragment, primarily located on the Sn atom bonded to palladium.

Although our system differs in several respects from that in Scheme 4, it nevertheless seemed of interest to calculate the p-orbital contribution of each of the two alkyne carbons to the occupied frontier π-orbital (the one delocalized with the substituents). These HOMO contributions were obtained by DFT calculations for models of most alkynes used in this study. Very similar p-orbital contributions were calculated when the geometries of the alkynes were altered to mimic that likely to be found in the transition state for insertion, i.e., with an angle of 145° between the substituents and the C_2 fragment instead of 180°.[39,40] The results, listed in Table 7, suggest that all the experimental regioselectivities can be accounted for by such a simple model. The major contributions for PhC≡CCO_2H and MeC≡CCO_2H are located on the carbon atom bearing the carboxylate group (entries 5 and 6); hence, interaction with an

(33) Klein, H.-F.; Reitzel, L. *Chem. Ber.* **1988**, *121*, 1115.
(34) Maassarani, F.; Pfeffer, M.; Le Borgne, G. *Organometallics* **1987**, *6*, 2029.
(35) Maassarani, F.; Pfeffer, M.; Le Borgne, G. *Organometallics* **1987**, *6*, 2043.
(36) Maassarani, F.; Pfeffer, M.; Le Borgne, G. *J. Chem. Soc., Chem. Commun.* **1987**, 565.
(37) Spencer, J.; Pfeffer, M.; DeCian, A.; Fischer, J. *J. Org. Chem.* **1995**, *60*, 1005.
(38) (a) Lohner, P.; Pfeffer, M.; de Cian, A.; Fischer, J. *C. R. Acad. Sci. Paris, Ser. IIc* **1998**, 615. (b) Pfeffer, M. Personal communication.
(39) Hada, M.; Tanaka, Y.; Ito, M.; Murakami, M.; Amii, H.; Ito, Y.; Nakatsuji, H. *J. Am. Chem. Soc.* **1994**, *116*, 8754.
(40) Macgregor, S. A.; Wenger, E. Manuscript in preparation.

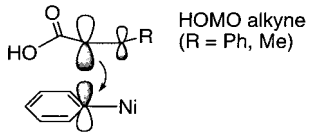

Figure 8.

Table 7. Computed Alkyne Carbon p-Orbital Contributions (%) to the Delocalized Occupied Frontier Orbitals of $R^1C^1{\equiv}C^2R^2$

entry	R^1	R^2	C^1	C^2
1	H	Me	48.0	40.3
2	H	Ph	29.1	12.6
3	H	SiH_3	43.4	41.0
4	Me	Ph	27.5	16.5
5	CO_2H	Ph	25.9	8.5
6	CO_2H	Me	41.1	32.9
7	CO_2H	CF_3	29.5	32.5
8	CO_2H	H	38.2	38.6

empty orbital located on the carbon atom bonded to nickel will lead to seven-membered complexes with the carboxylate groups adjacent to the phenyl ring. An illustration of such an interaction is given in Figure 8. For $CF_3C{\equiv}CCO_2H$ a reversal of polarity in the alkyne orbital is computed, consistent with the change in regioselectivity observed experimentally. The regioselectivities observed for the insertions of PhC≡CH and PhC≡CMe can also be explained by similar electronic arguments. The large p-orbital contributions for these two alkynes are located on ≡CH and ≡CMe, respectively (entries 2 and 4 of Table 7), hence leading to products that have the phenyl groups adjacent to the metal.

In the case of the alkynylphosphines, the regioselectivity can be best rationalized by coordination of the phosphine group to the metal during the insertion step, leading to formation of the bicyclic species **16**, **18a**,**b**, and **20** (Scheme 3). Because of the strain of the three-membered nickelacycles, these complexes tend to rearrange rapidly, either by internal migration of a substituent as for **18b** and **20** or by reaction with a neighboring complex to form a dimer such as **17**. As the primary objective of this work was to determine the regioselectivities of the insertion reactions, the mechanisms of these subsequent rearrangements have not been investigated further.

Conclusion

The insertions of alkynes into the Ni−C bonds of the nickelacycles **2a** and **2b** seem to be governed mainly by electronic factors, possibly a frontier orbital interaction between the alkyne and the Ni−C bond. It is possible to rationalize the observed regioselectivities on the basis of a simple model in which the HOMO of the alkyne overlaps with a LUMO located on the carbon atom of the Ni−C bond. However, this model is purely empirical and does not provide a precise description of the interaction of the coordinated alkyne with the Ni−C bond that would account for both reactivity and regioselectivity. Moreover, the regioselectivities established for **2a**,**b** cannot be simply carried over to the benzyne−nickel chemistry that prompted this work (see Introduction), as in the latter system methyl propynoate and methyl 2-butynoate do not give products with opposite regiochemistry.[22−24] The reason for this difference may be due to the presence of the electron-withdrawing bromide in **2a**,**b**. More detailed DFT computational studies investigating all these issues are underway.[40]

Experimental Section

General Procedures. All experiments, unless otherwise specified, were carried out under argon using standard Schlenk techniques. All solvents were dried and degassed prior to use. NMR spectra were recorded on a Varian XL-200E (^{1}H at 200 MHz, ^{13}C at 50.3 MHz, ^{31}P at 81.0 MHz), a Varian Gemini 300BB or Varian Mercury 300 (^{1}H at 300 MHz, ^{13}C at 75.4 MHz, ^{31}P at 121.4 MHz), or a Varian Inova-500 instrument (^{1}H at 500 MHz, ^{13}C at 125.7 MHz). The chemical shifts (δ) for ^{1}H and ^{13}C are given in ppm relative to residual signals of the solvent and to external 85% H_3PO_4 for ^{31}P. The spectra of all nuclei (except ^{1}H) were ^{1}H-decoupled. The coupling constants (J) are given in Hz. The regioselectivities were investigated by use of the GOESY pulse sequence on the Inova-500 spectrometer. Infrared spectra were measured on a Perkin-Elmer Spectrum One instrument. Mass spectra of the complexes were obtained on a ZAB-SEQ4F spectrometer by the fast-atom bombardment (FAB) technique or on a Micromass Tof Spec 2E instrument by the MALDI/TOF technique.

The products of the insertion reactions (**3**−**15**) were generally unstable and have been studied primarily in situ by multinuclear NMR spectroscopy (typically ca. 30−40 mg of complex **2a** or **2b** in 0.5 mL of C_6D_6 or CD_2Cl_2). However, the nickelacycles **4b**, **6b**, and **10b**, having PBz_2Ph as the auxiliary ligand, could be crystallized and microanalytical data were obtained in house. Single crystals for the rearrangement products **17** and **21** were also isolated from NMR scale reactions, but in these cases, not enough material could be isolated to obtain microanalyses.

Starting Materials. The (alkynyl)diphenylphosphines $Ph_2PC{\equiv}CR$ (R = Me, Ph, CO_2Me)[41−43] and the fluoro alkyne $CF_3C{\equiv}CCO_2Et$[44] were prepared by following published procedures. The complexes [NiBr($C_6H_4CH_2PPh_2$)(PR_3)] (PR_3 = PEt_3 (**2a**), $PPhBz_2$ (**2b**)) were prepared by reaction of [Ni(cod)$_2$][45] with *o*-$BrC_6H_4CH_2PPh_2$[46] in the presence of 1 equiv of the corresponding tertiary phosphine, as described by Muller.[25]

2a. ^{1}H NMR (300 MHz, CD_2Cl_2): δ 1.20 ([A_3BCX] m, 9H, J = 5, CH_3^{PEt}), 1.79 ([A_3BCX] m, 6H, J = 5, CH_2^{PEt}), 3.86 (dd, 2H, $^2J_{HP}$ = 6.0, $^4J_{HP}$ = 1.3, CH_2PPh$_2$), 6.75 (t, 1H, J = 4.7, H^{Ph}), 6.82 (t, 1H, J = 4.7, H^{Ph}), 6.97 (d, 1H, J = 4.7, H^{Ph}), 7.15 (d, 1H, J = 4.7, H^{Ph}), 7.35−7.60 (m, 6H, PPh_2), 7.78 (t, 4H, J = 5.5, PPh_2). ^{13}C{^{1}H} NMR (75.4 MHz, CD_2Cl_2): δ 8.42 (CH_3), 16.19 (d, J_{CP} = 22.0, CH_2), 43.35 (d, J_{CP} = 32.9, CH_2), 123.59, 123.79, 124.20, 124.39 (CH^{Ph}), 128.35 (d, J_{CP} = 9.9, CH^{PPh}), 130.49 (CH^{PPh}), 133.04 (d, J_{CP} = 9.9, CH^{PPh}), 139.22 (d, J_{CP} = 14.3, C^{PPh}), 147.60 (d, J_{CP} = 21.9, C^2), 152.77 (app t, J_{CP} = 24.1, C^1−Ni). ^{31}P{^{1}H} NMR (81.0 MHz, C_6D_6): δ 11.8 (d), 44.5 (d, $^2J_{PP}$ = 343.2).

2b. ^{1}H NMR (200 MHz, CD_2Cl_2): δ 3.32 (br t, 2H, J_{HP} = 11.5, CH_2PPh$_2$), 3.68 (br d, 4H, J_{HP} = 8.6, CH_2Ph), 6.02 (d, 1H, J = 7.5, H^{Ph}), 6.17 (t, 1H, J = 7.5, H^{Ph}), 6.60 (t, 1H, J = 7.5, H^{Ph}), 6.82 (d, 1H, J = 7.5, H^{Ph}), 7.15−7.60 (m, 6H, PPh_2), 7.79 (t, 4H, J = 8.3, PPh_2). ^{13}C{^{1}H} NMR (75.4 MHz, CD_2Cl_2): δ 32.16 (d, J_{CP} = 18.4, CH_2Ph), 43.22 (d, J_{CP} = 32.5, CH_2PPh$_2$), 123.54, 123.76, 124.28, 124.35 (CH^{Ph}), 126.77 (CH^{PPh}), 128.19 (d, J_{CP} = 9.1, CH^{PPh}), 128.41 (CH^{PPh}), 128.64 (d, J_{CP} = 9.5, CH^{PPh}), 130.17 (CH^{PPh}), 130.47 (d, J_{CP} = 5.1, CH^{PPh}), 130.80 (CH^{PPh}), 132.36 (dd, J_{CP} = 36.4, 4.0, C^{PPh}), 133.36 (d, J_{CP} =

(41) Charrier, C.; Chodkiewicz, W.; Cadiot, P. *Bull. Soc. Chim. Fr.* **1966**, 1002.
(42) Carty, A. J.; Hota, N. K.; Ng, T. W.; Patel, H. A.; O'Connor, T. J. *Can. J. Chem.* **1971**, *49*, 2706.
(43) Montlo, D.; Suades, J.; Dahan, F.; Mathieu, R. *Organometallics* **1990**, *9*, 2933.
(44) Hamper, B. C. *Org. Synth.* **1992**, *70*, 246.
(45) Schunn, R. A. *Inorg. Synth.* **1974**, *15*, 5.
(46) Abicht, H.-P.; Issleib, K. *Z. Anorg. Allg. Chem.* **1976**, *422*, 237.

9.4, CH^{PPh}), 133.69 (d, J_{CP} = 10.0, CH^{PPh}), 135.42 (d, J_{CP} = 3.1, C^{PBz}), 140.47 (d, J_{CP} = 12.6, C^{PPh2}), 147.46 (d, J_{CP} = 21.5, C^2), 151.80 (m, C^1−Ni). $^{31}P\{^1H\}$ NMR (81.0 MHz, CD_2Cl_2): δ 17.1 (d), 47.6 (d, $^2J_{PP}$ = 336.1). FAB-MS (nitrophenyl octyl ether, $C_{39}H_{35}BrNiP_2$): *m/z* 705 (42, MH^+), 624 (100, MH^+ − Br).

Reaction of 2a with PhC≡CCO$_2$Et. In a typical experiment, an NMR solution of **2a** (36 mg, 0.068 mmol) in C_6D_6 (0.6 mL) was prepared under N_2 at 5 °C, and ethyl phenylpropynoate (0.013 mL, 0.08 mmol) was added. ^{31}P NMR monitoring showed the reaction to be quantitative after 10 min at room temperature, forming only one insertion product (**3a**). ^1H NMR (500 MHz, C_6D_6): δ 0.66 (t, 3H, J_{HH} = 7.0, CH_3), 0.70 ([A_3BCX] m, 9H, J = 7.5, $CH_3{}^{PEt}$), 1.62 ([A_3BCX] m, 3H, J = 7.5, $CH_2{}^{PEt}$), 1.70 ([A_3BCX] m, 3H, J = 7.5, $CH_2{}^{PEt}$), 2.79 (app dt, 1H, $^2J_{HH}$ = $^2J_{HP}$ = 12.0, $^4J_{HP}$ = 2.0, CH_2PPh_2), 3.74−3.88 (m, 2H, OCH_2), 4.02 (dd, 1H, $^2J_{HH}$ = 12.0, $^2J_{HP}$ = 9.0, CH_2PPh_2), 6.41 (d, 1H, J_{HH} = 7, H^3), 6.73−7.10 (m, 10H), 7.18 (t, 1H, J_{HH} = 7, H^{4or5}), 7.61 (dt, 2H, J = 2, 10, H^{PPh}), 7.63 (dd, 2H, J = 8, 1.7, H^{Ph}), 7.87 (d, 1H, J_{HH} = 7, H^6), 8.08 (t, 2H, J = 8, H^{PPh}). GOESY (500 MHz, C_6D_6): irradiation at δ 3.74−3.88 gave responses from δ 0.66 and 7.63; irradiation at δ 0.70 gave responses from δ 1.62, 1.70, 3.55, 7.61, 7.63, and 7.87; irradiation at δ 1.50−1.75 gave responses from δ 0.70, 7.63, and 7.87. $^{13}C\{^1H\}$ NMR (75.4 MHz, C_6D_6): δ 7.56 (CH_3), 13.87 (CH_3), 14.60 (d, J_{CP} = 23, CH_2), 32.96 (d, J_{CP} = 26.3, CH_2), 60.15 (OCH_2), 126.57, 126.79, 126.95, (CH), 127.18 (d, J_{CP} = 3.3, CH), 127.27 (br s, C^{vinyl}), 127.53 (d, J_{CP} = 7.7, CH), 128.80 (d, J_{CP} = 8.8, CH^{PPh}), 129.87 (d, J_{CP} = 2.2, CH^{PPh}), 130.04 (CH), 130.31 (d, J_{CP} = 2.2, CH^{PPh}), 130.86 (d, J_{CP} = 4.4, CH^{PPh}), 131.90 (dd, J_{CP} = 28.5, 4.4, C^{PPh}), 132.73 (dd, J_{CP} = 13.0, 6.6, C^{Ph}), 132.98 (d, J_{CP} = 7.7, CH^{PPh}), 134.97 (d, J_{CP} = 9.9, CH^{PPh}), 135.44 (d, J_{CP} = 42.6, C^{PPh}), 142.23 (C^1), 143.39 (d, J_{CP} = 3.3, C^2), 166.17 (dd, J_{CP} = 5.2, 2.5, CO), 173.91 (dd, J_{CP} = 30.7, 25.2, C−Ni). $^{31}P\{^1H\}$ NMR (81.0 MHz, C_6D_6): δ 6.9 (d), 27.5 (d, $^2J_{PP}$ = 301.7).

Reaction of 2a with MeC≡CCO$_2$Me. A suspension of **2a** (58 mg, 0.11 mmol) in ether (5 mL) was treated with methyl 2-butynoate (0.014 mL, 0.13 mmol) at 0 °C. After 1 h at room temperature, the solvent was evaporated and the ^{31}P NMR spectrum of the yellow solid showed the reaction to be quantitative, as only one phosphorus-containing compound (**4a**) was present. ^1H NMR (500 MHz, CD_2Cl_2): δ 1.03 ([A_3BCX] m, 9H, J = 7.5, $CH_3{}^{PEt}$), 1.62 ([A_3BCX] m, 3H, J = 7.5, $CH_2{}^{PEt}$), 1.80 ([A_3BCX] m, 3H, J = 7.5, $CH_2{}^{PEt}$), 2.44 (dd, 3H, J_{HP} = 2.0, 1.5, CH_3), 3.02 (app dt, 1H, $^2J_{HH}$ = $^2J_{HP}$ = 12.0, $^4J_{HP}$ = 2.0, CH_2PPh_2), 3.48 (dd, 1H, $^2J_{HH}$ = 12.0, $^2J_{HP}$ = 9.0, CH_2PPh_2), 3.55 (s, 3H, OMe), 6.73 (d, 1H, J = 7.5, H^3), 7.16 (t, 1H, J = 7.5, H^{4or5}), 7.26−7.31 (m, 6H, H^{PPh}), 7.34 (t, 1H, J = 7.5, H^{5or4}), 7.57−7.62 (m, 3H, H^{6+PPh}), 8.11−8.15 (m, 2H, H^{PPh}). GOESY (500 MHz, CD_2Cl_2): irradiation at δ 1.03 gave responses from δ 1.62, 1.80, 2.44, and 7.30; irradiation at δ 2.44 gave responses from δ 1.03, 1.62, 1.80, 3.55, and 8.13. $^{13}C\{^1H\}$ NMR (75.4 MHz, C_6D_6): δ 8.11 (CH_3), 14.83 (d, J_{CP} = 28.8, CH_2), 24.80 (d, J_{CP} = 7.6, CH_3), 33.18 (d, J_{CP} = 29.6, CH_2), 50.41 (OMe), 126.15 (d, J_{CP} = 2.2, CH), 126.63 (br s, C^{vinyl}), 127.03 (d, J_{CP} = 3.3, CH), 127.62 (d, J_{CP} = 8.8, CH^{PPh}), 128.99 (d, J_{CP} = 8.8, CH^{PPh}), 129.79 (CH), 130.49 (CH), 130.59 (d, J_{CP} = 2.2, CH^{PPh}), 130.76 (d, J_{CP} = 4.4, CH^{PPh}), 131.09 (dd, J_{CP} = 31.0, 3.6, C^{PPh}), 133.07 (d, J_{CP} = 9.9, CH^{PPh}), 133.79 (C^1), 134.05 (d, J_{CP} = 9.9, CH^{PPh}), 135.60 (dd, J_{CP} = 37.3, 1.4, C^{PPh}), 143.66 (d, J_{CP} = 1.9, C^2), 162.22 (dd, J_{CP} = 5.2, 2.2, CO), 197.00 (dd, J_{CP} = 31.9, 25.2, C−Ni). $^{31}P\{^1H\}$ NMR (81.0 MHz, CD_2Cl_2): δ 9.4 (d), 29.0 (d, $^2J_{PP}$ = 274.6). EI-MS ($C_{30}H_{37}BrNiO_2P_2$) *m/z* 629 (1, M^+ − H), 549 (3, M^+ − Br), 471 (3), 373 (100, $C_6H_4(PPh_2)(C(CO_2Me)$=$CMe)$).

Reaction of 2a with HC≡CCO$_2$Me. Treatment of **2a** (42 mg, 0.079 mmol) with 1.1 equiv of HC≡CCO_2Me at −78 °C in CD_2Cl_2 (0.5 mL), followed by warming to room temperature, gave **6a** as the major insertion product, containing only a trace (<8%) of the second isomer **7a**, together with some cyclotrimerization products.[47] Attempted purification by crystallization led to decomposition.

6a. ^1H NMR (300 MHz, CD_2Cl_2): δ 1.04 ([A_3BCX] m, 9H, J = 7.5, $CH_3{}^{PEt}$), 1.63 ([A_3BCX] m, 3H, J = 7.5, $CH_2{}^{PEt}$), 1.75 ([A_3BCX] m, 3H, J = 7.5, $CH_2{}^{PEt}$), 3.09 (app dt, 1H, $^2J_{HH}$ = $^2J_{HP}$ = 12.0, $^4J_{HP}$ = 2.0, CH_2PPh_2), 3.51 (dd, 1H, $^2J_{HH}$ = 12.0, $^2J_{HP}$ = 10.0, CH_2PPh_2), 3.60 (s, 3H, OMe), 6.69 (br t, J = 7, H^{vinyl}), 6.86 (d, 1H, J = 7.5, H^3), 6.90−7.84 (m, 14H, H^{arom}), 8.15−8.24 (m, 2H, H^{PPh}). GOESY (500 MHz, CD_2Cl_2): irradiation at δ 1.00−1.30 gave responses from δ 1.65, 1.77, 3.64, and 7.33. $^{13}C\{^1H\}$ NMR (50.2 MHz, C_6D_6): δ 7.97 (CH_3), 14.98 (d, J_{CP} = 23.1, CH_2), 27.96 ($CH_3{}^{Bu}$), 33.44 (d, J_{CP} = 29.8, CH_2), 80.25 (C^{Bu}), 126.07 (br s, CH), 126.80 (d, J_{CP} = 3, CH), 127.34 (d, J_{CP} = 9.4, CH^{PPh}), 128.25−132.60 (m, CH + C), 133.25 (d, J_{CP} = 8.8, CH^{PPh}), 136.32 (d, J_{CP} = 37.1, C^{PPh}), 141.64 (C), 141.97 (t, J_{CP} = 6.3, CH^{vinyl}), 149.05 (dd, J_{CP} = 38.7, 30.7, Ni−C), 167.53 (C), 170.46 (br s, CO). $^{31}P\{^1H\}$ NMR (81.0 MHz, CD_2Cl_2): δ 9.3 (d), 30.9 (d, $^2J_{PP}$ = 321.8).

7a. $^{31}P\{^1H\}$ NMR (81.0 MHz, CD_2Cl_2): δ 13.9 (d), 33.8 (d, $^2J_{PP}$ = 294.0).

Reaction of 2a with HC≡CCO$_2{}^t$Bu. A solution of **2a** (33 mg, 0.062 mmol) in CD_2Cl_2 (0.5 mL) was treated with HC≡$CCO_2{}^t$Bu (1 equiv). After 2 days, ^{31}P NMR monitoring showed a 5:1 mixture of the two insertion isomers **8a** and **9a** (>90% total yield).

8a. ^1H NMR (500 MHz, CD_2Cl_2): δ 0.90−1.80 (m, 15H, PEt_3), 1.32 (s, 6H, ^{t}Bu), 1.40 (s, 3H, ^{t}Bu), 2.93 (dt, 1H, $^4J_{HP}$ = 2.0, $^2J_{HH}$ = $^2J_{HP}$ = 12.0, CH_2PPh_2), 3.54 (dd, 1H, $^2J_{HH}$ = 12.0, $^2J_{HP}$ = 9.2, CH_2PPh_2), 4.22−4.35 (m, 1H, H^{vinyl}), 6.62 (d, 1H, J = 7.3, H^3), 7.08 (t, 1H, J = 7.5, H^{4or5}), 7.20−7.70 (m, 9H, H^{arom}), 8.05−8.20 (m, 3H, H^{arom}). $^{13}C\{^1H\}$ NMR (50.2 MHz, C_6D_6): δ 7.91 (CH_3), 14.75 (d, J_{CP} = 24.2, CH_2), 33.85 (d, J_{CP} = 29.7, CH_2), 51.20 (OMe), 126.50 (CH), 127.16 (br s, CH), 127.65 (d, J_{CP} = 8.8, CH^{PPh}), 128.25−132.60 (m, CH + C), 132.99 (d, J_{CP} = 8.8, CH^{PPh}), 134.19 (d, J_{CP} = 9.9, CH^{PPh}), 136.00 (dd, J_{CP} = 36.5, 1.6, C^{PPh}), 140.86 (t, J_{CP} = 6.3, CH^{vinyl}), 141.50 (C), 150.80 (dd, J_{CP} = 38.3, 31.4, C−Ni), 167.53 (C), 168.69 (dd, J_{CP} = 4.4, 2, CO). $^{31}P\{^1H\}$ NMR (81.0 MHz, CD_2Cl_2): δ 7.7 (d), 29.4 (d, $^2J_{PP}$ = 324.8).

9a. $^{31}P\{^1H\}$ NMR (81.0 MHz, CD_2Cl_2): δ 13.9 (d), 34.0 (d, $^2J_{PP}$ = 297.1).

Reaction of 2a with HC≡CPh. Treatment of a NMR solution of **2a** (29 mg, 0.054 mmol) in C_6D_6 (0.5 mL) with HC≡CPh (7.2 μL, 1.1 equiv) gave a dark red solution with only one major insertion product (**12a**), as shown by ^{31}P NMR monitoring. The reaction however was not very clean, and any attempts to purify **12a** led to decomposition.

12a. $^{31}P\{^1H\}$ NMR (81.0 MHz, CD_2Cl_2): δ 6.3 (d), 26.1 (d, $^2J_{PP}$ = 308.5).

Reaction of 2a with HC≡C^{t}Bu. *tert*-Butylacetylene (11 μL, 0.09 mmol) was added to a solution of **2a** (48 mg, 0.09 mmol) in CD_2Cl_2 (0.6 mL) at −78 °C. After 10 min at room temperature, ^{31}P NMR monitoring showed that **2a** had completely reacted and that only one insertion product (**11a**) was present, together with traces of decomposition. Attempts to isolate and purify the complex led to further decomposition.

11a. $^{13}C\{^1H\}$ NMR (75.4 MHz, CD_2Cl_2): δ 8.34 (d, J_{CP} = 3.3, CH_3), 15.96 (d, J_{CP} = 22.0, CH_2), 30.09, 30.30, 32.26 ($CH_3{}^{tBu}$), 33.97 (d, J_{CP} = 31.8, CH_2), 42.08 (C^{tBu}), 51.20 (OMe), 123.70−132.80 (m, CH + C), 133.18 (t, J_{CP} = 7.7, CH), 133.76 (d, J_{CP} = 8.8, CH^{PPh}), 136.79 (d, J_{CP} = 36.2, C^{PPh}), 137.22 (d, J_{CP} = 8.8, C), 138.72 (d, J_{CP} = 4.4, C), 143.44 (C), 170.75 (d, J_{CP} = 26.4, C), 173.88 (dd, J_{CP} = 36.2, 24.1, C−Ni). $^{31}P\{^1H\}$ NMR (81.0 MHz, CD_2Cl_2): δ 0.7 (d), 19.8 (d, $^2J_{PP}$ = 319.4).

Reaction of 2a with HC≡CSiMe$_3$. An NMR-scale reaction of **2a** (42 mg, 0.079 mmol) with 1 equiv of HC≡$CSiMe_3$ in CD_2Cl_2 (0.6 mL) gave only traces of an insertion product (**13a**), together with starting material and some decomposition. Addition of an excess of alkyne led to complete decomposition.

(47) Diercks, R.; tom Dieck, H. *Z. Naturforsch.* **1984**, *B39*, 180.

13a. $^{31}P\{^{1}H\}$ NMR (81.0 MHz, CD_2Cl_2): δ 4.5 (d), 26.1 (d, $^{2}J_{PP} = 312$).

Reaction of 2a with $MeO_2CC{\equiv}CPPh_2$. As described above, a solution of **2a** (34 mg, 0.064 mmol) in C_6D_6 (0.6 mL) was treated with 1.2 equiv of $MeO_2CC{\equiv}CPPh_2$. Monitoring by ^{31}P NMR spectroscopy showed formation of one major compound (**16**; >90%). Crystallization from CH_2Cl_2/pentane yielded orange crystals of the rearrangement product **17**, whose dimeric structure was confirmed by X-ray analysis.

16. ^{1}H NMR (300 MHz, CD_2Cl_2): δ 0.69 ([A_3BCX] m, 9H, $J = 7.5$, $CH_3{}^{PEt}$), 1.37 ([A_3BCX] m, 6H, $J = 7.5$, $CH_2{}^{PEt}$), 3.35 (s, 3H, OMe), 3.41 (br d, 1H, $J = 8.5$, CH_2PPh_2), 4.22−4.35 (m, 1H, CH_2PPh_2), 6.17 (d, 1H, $J = 8$, H^3), 7.16 (dt, 1H, $^{4}J = 1$, $^{3}J = 8$, H^{4or5}), 7.00−7.90 (m, 22H, H^{arom}). $^{13}C\{^{1}H\}$ NMR (75.4 MHz, C_6D_6): δ 8.31 (d, $J_{CP} = 3.3$, CH_3), 17.90 (dd, $J_{CP} = 19.8$, 1.8, CH_2), 39.38 (dd, $J_{CP} = 22$, 5.5, CH_2), 51.41 (OMe),125.95, 126.29 (CH),128.1−130.4 (m, CH + C), 130.84 (CH), 131.17 (m, C), 1303.91 (d, $J_{CP} = 12.1$, CH^{PPh}), 138.29 (dd, $J_{CP} = 10$, 4.3, C), 162.90 (dd, $J_{CP} = 13.2$, 3.3, CO), 170.0−171.10 (m, C−Ni). $^{31}P\{^{1}H\}$ NMR (121.4 MHz, CD_2Cl_2): δ −101.5 (dd, $^{2}J_{PP} = 239.0$, 42.6, PPh_2), 13.8 (dd, $^{2}J_{PP} = 42.8$, 27.9, PEt_3), 28.6 (dd, $^{2}J_{PP} = 239$, 27.9, CH_2PPh_2).

17. $^{31}P\{^{1}H\}$ NMR (81.0 MHz, CD_2Cl_2): δ 29.6 (br s), 19.3 (br s).

Reaction of 2a with $MeC{\equiv}CPPh_2$. A solution of **2a** (26 mg, 0.049 mmol) in CD_2Cl_2 (0.5 mL) was treated with 1.2 equiv of $MeC{\equiv}CPPh_2$. After 16 h at room temperature, ^{31}P NMR monitoring showed the main compound to be [NiBr{*o*-$C(PPh_2){=}C(Me)C_6H_4CH_2PPh_2$}($PEt_3$)] (**18a**). Attempted isolation led to decomposition.

18a. $^{31}P\{^{1}H\}$ NMR (81.0 MHz, CD_2Cl_2): δ −112.9 (dd, $^{2}J_{PP} = 238.0$, 40.0, PPh_2), 13.9 (dd, $^{2}J_{PP} = 40.3$, 20.5, PEt_3), 29.7 (br d, $^{2}J_{PP} = 234.1$, CH_2PPh_2).

Reaction of 2b with $MeC{\equiv}CCO_2Me$. A solution of **2b** (30 mg) in CD_2Cl_2 (0.5 mL) was treated with 1.2 equiv of $MeC{\equiv}CCO_2Me$ at −78 °C. Monitoring by ^{31}P NMR spectroscopy showed the reaction to be quantitative after 5 min at room temperature, giving a mixture of the two regioisomers **4b** and **5b** in a 3.2:1 ratio.

In another experiment in thf (0.5 mL)/C_6D_6 (0.1 mL), the quantitative insertion gave a 7:1 mixture of **4b** and **5b**. Cooling of the solution gave yellow X-ray-quality single crystals of **4b**.

4b. IR (KBr): 3010 (w), 2922 (m), 1695 (vs, ν_{CO}), 1597 (m), 1536 (m), 1432 (s), 1268 (s), 1218 (vs), 1099 (s), 1030 (s), 779 (s), 739 (s), 693 (vs),509 (m), 493 (m) cm^{-1}. ^{1}H NMR (300 MHz, CD_2Cl_2): δ 1.77 (br s, 3H, CH_3), 2.99 (dd, 1H, $J = 15$, 5.2, $CH_2{}^{PBz}$), 3.02 (dt, 1H, $J = 1$, 12.2, CH_2P), 3.12 (ddd, 1H, $J = 15.5$, 13.1, 4.3, $CH_2{}^{PBz}$), 3.33 (dd, 1H, $J = 14.3$, 5.5, $CH_2{}^{PBz}$), 3.47 (s, 3H, OMe), 3.55 (dd, 1H, $J = 12.1$, 9.2, CH_2P), 3.98 (dd, 1H, $J = 12.8$, 9.2, $CH_2{}^{PBz}$), 6.71 (d, 2H, $J = 7$, H^{Ph}), 6.81 (d, 1H, $J = 7.6$, H^3), 6.99 (t, 2H, $J = 8$, H^{Ph}), 7.06−7.48 (m, 17H, H^{Ph}), 7.58−7.64 (m, 3H, H^{6+PPh}), 7.94 (d, 2H, $J = 7.4$, H^{Ph}), 8.07−8.15 (m, 2H, H^{PPh}). GOESY (500 MHz, CD_2Cl_2): irradiation at δ 2.92−2.97 gave responses from δ 1.82 (s), 3.37 (dd), 6.76 (d), and 7.98 (d); irradiation at δ 1.80 gave responses from δ 2.96 (dd), 7.99 (d), and 8.16 (m). $^{13}C\{^{1}H\}$ NMR (75.4 MHz, C_6D_6): δ 23.98 (d, $J_{CP} = 6.5$, CH_3), 25.80 (d, $J_{CP} = 22$, CH_2), 29.61 (d, $J_{CP} = 15.3$, CH_2), 33.35 (d, $J_{CP} = 30.7$, CH_2PPh_2), 50.92 (OMe), 126.64 (br s, CH), 127.29 (br s, CH), 127.60−131.50 (m, CH + C), 132.73 (C), 132.96 (d, $J_{CP} = 9.9$, CH^{PPh}), 133.30 (d, $J_{CP} = 9.9$, CH^{PPh}), 133.69 (d, $J_{CP} = 9.9$, CH^{PPh}), 133.93−134.81 (m, C), 135.60 (dd, $J_{CP} = 37.3$, 1.4, C^{PPh}), 143.43 (dd, $J_{CP} = 2.8$, 1.6, C), 162.22 (dd, $J_{CP} = 5.5$, 2.3, CO), 195.77 (dd, $J_{CP} = 31.3$, 24.5, C−Ni). $^{31}P\{^{1}H\}$ NMR (81.0 MHz, CD_2Cl_2): δ 10.6 (d), 31.7 (d, $^{2}J_{PP} = 282.1$). Anal. Calcd for $C_{44}H_{41}BrNiO_2P_2{\cdot}{}^{1}/_{2}CH_2Cl_2$: C, 63.27; H, 5.01. Found: C, 63.47; H, 5.30.

5b. $^{31}P\{^{1}H\}$ NMR (81.0 MHz, CD_2Cl_2): δ 9.5 (d), 32.4 (d, $^{2}J_{PP} = 333.7$).

Reaction of 2b with $F_3CC{\equiv}CCO_2Et$. A suspension of **2b** (126 mg, 0.18 mmol) in ether (15 mL) was treated with $F_3CC{\equiv}CCO_2Et$ (26 μL, 0.18 mmol) at −78 °C. After the mixture was warmed to room temperature, monitoring of the orange solution by ^{31}P NMR spectroscopy showed the reaction to be quantitative. After filtration through Celite, the solvent was removed in vacuo. Crystallization from chlorobenzene/pentane was accompanied by decomposition and gave orange-red single crystals of **10b** (28 mg, 18%) of mediocre quality.

10b. IR (KBr): 3056 (m), 2996 (w), 1697 (s, ν_{CO}), 1597 (m), 1433 (s), 1301 (s, ν_{CF}), 1185 (vs), 1088 (vs), 696 (s), 523 (m), 510 (m), 492 (m), 477 (m) cm^{-1}. ^{1}H NMR (300 MHz, CD_2Cl_2): δ 0.83 (t, 3H, $J = 7.2$, CH_3), 3.04 (dt, 1H, $J = 13$, 3, CH_2P), 3.32 (dt, 1H, $J = 15.5$, 3, CH_2P), 3.48 (dd, 1H, $J = 15.5$, 8, CH_2P), 3.66 (m, 1H, OCH_2), 3.76 (dd, 1H, $J = 12$, 8.8, CH_2P), 3.81 (dd, 1H, $J = 15$, 6, CH_2P), 3.83 (m, 1H, OCH_2), 3.86 (app t, $J = 11.8$, CH_2P), 6.58 (d, 1H, $J = 7.8$, H^{Ph}), 6.89 (d, 2H, $J = 7.5$, H^{Ph}), 7.03−7.67 (m, 24H, H^{Ph}), 8.18 (ddd, 2H, $J = 9.9$, 8.4, 2.1, H^{Ph}). $^{13}C\{^{1}H\}$ NMR (75.4 MHz, CD_2Cl_2): δ 13.83 (CH_3), 27.14 (d, $J_{CP} = 23.7$, CH_2), 31.56 (d, $J_{CP} = 18.1$, CH_2), 32.47 (d, $J_{CP} = 29.9$, CH_2PPh_2), 60.73 (OCH_2), 120.44 (qdd, $J_{CF} = 277.2$, $J_{CP} = 5.1$, 3.2, CF_3), 126.60−134.90 (m, CH + C), 137.57 (C), 140.33 (br, C), 165.24 (ddq, $J_{CP} = 32.5$, 28.2, $J_{CF} = 2.5$, C−Ni), 169.81 (d, $J_{CP} = 3.8$, CO). $^{31}P\{^{1}H\}$ NMR (81.0 MHz, C_6D_6): δ 9.2 (dq, $^{2}J_{PP} = 318.6$, $^{4}J_{PF} = 4.7$), 32.2 (dq, $^{2}J_{PP} = 318.6$, $^{4}J_{PF} = 5.2$). FAB-MS (nitrophenyl octyl ether, $C_{45}H_{40}BrF_3NiO_2P_2$) *m*/*z* 790 (18, $MH^+ - Br$), 441 (100, $C_6H_4(CH_2PPh_2)\{C(CF_3){=}C(CO_2Et)\}^+$). Anal. Calcd for $C_{45}H_{40}BrF_3NiO_2P_2$: C, 62.10; H, 4.63. Found: C, 61.19; H, 4.72.

Reaction of 2b with $HC{\equiv}CCO_2Me$. Methyl propynoate (30 μL, 0.34 mmol) was added to a solution of **2b** (239 mg, 0.34 mmol) in CH_2Cl_2 at −78 °C. The solution was warmed to room temperature over 1 h. ^{31}P NMR monitoring of the dark red solution showed the reaction to be quantitative and that the two isomers **6b** and **7b** were present in a 9:1 ratio. The solvent was removed in vacuo. Crystallization from toluene/pentane was accompanied by decomposition but afforded 31 mg (12%) of orange crystals of **6b** suitable for X-ray analysis.

6b. IR (CH_2Cl_2): 3032 (m), 1688 (s, ν_{CO}), 1601 (m), 1495 (s), 1203 (vs), 828 (m), 499 (s), 470 (s) cm^{-1}. ^{1}H NMR (500 MHz, CD_2Cl_2) δ 3.08−3.18 (m, 2H, PCH_2), 3.28−3.42 (m, 2H, PCH_2), 3.32 (s, 3H, OMe), 3.63 (br t, 1H, $J = 11$, PCH_2), 3.83 (dd, 1H, $J = 13.7$, 8, PCH_2), 6.82 (d, 1H, $J = 7$, H^{Ph}), 6.87 (d, 2H, $J = 6.5$, H^{Ph}), 7.11 (t, 2H, $J = 6.8$, H^{Ph}), 7.12−7.66 (m, 23H), 8.24 (br t, 2H, $J = 7.2$, H^{Ph}). $^{13}C\{^{1}H\}$ NMR (50.3 MHz, CD_2Cl_2): δ 27.57 (d, $J_{CP} = 21.4$, CH_2), 30.75 (d, $J_{CP} = 17.8$, CH_2), 34.53 (d, $J_{CP} = 30.6$, CH_2PPh_2), 51.34 (OMe), 126.58 (d, $J_{CP} = 2$, CH), 126.76 (d, $J_{CP} = 2.3$, CH), 126.88 (d, $J_{CP} = 2$, CH), 127.60−132.00 (m, CH + C), 132.90 (d, $J_{CP} = 9.5$, CH^{PPh}), 133.38 (d, $J_{CP} = 10.1$, CH^{PPh}), 134.11 (dd, $J_{CP} = 9.6$, 1.4, CH^{PPh}), 134.60 (d, $J_{CP} = 1.9$, C), 134.84 (dd, 7.8, 1.6, C), 135.58 (d, $J_{CP} = 1.5$, C), 135.90 (d, $J_{CP} = 10.1$, C^{PPh}), 141.15 (br, C), 141.94 (t, $J_{CP} = 5.8$, CH^{vinyl}), 149.25 (dd, $J_{CP} = 39.5$, 29.5, C−Ni), 170.69 (dd, $J_{CP} = 5.5$, 3.0, CO). $^{31}P\{^{1}H\}$ NMR (81.0 MHz, CD_2Cl_2): δ 5.4 (d), 31.8 (d, $^{2}J_{PP} = 328.6$). Anal. Calcd for $C_{43}H_{39}BrNiO_2P_2$: C, 65.51; H, 4.99; P, 7.86. Found: C, 65.50; H, 5.02; P, 7.70.

7b. $^{31}P\{^{1}H\}$ NMR (81.0 MHz, CD_2Cl_2): δ 10.3 (d), 36.6 (d, $^{2}J_{PP} = 300.3$).

Reaction of 2b with $HC{\equiv}CPh$. Treatment of **2b** (56 mg, 0.08 mmol) with $HC{\equiv}CPh$ (9 μL, 0.08 mmol) in CD_2Cl_2 (0.6 mL) led to the formation of one insertion product (**12b**), as shown by ^{31}P NMR spectroscopy. This very sensitive complex decomposed overnight.

12b. ^{1}H NMR (300, CD_2Cl_2): δ 2.85−3.05 (m, 2H, CH_2), 3.10−3.20 (m, 1H, CH_2), 3.30−3.45 (m, 2H, CH_2), 3.85−3.405 (m, 1H, CH_2), 6.53 (br, 1H, H^{arom}), 6.84 (br, 2H, H^{arom}), 6.90−7.70 (m, 28H, H^{arom}), 7.76 (br, 2H, H^{arom}), 8.10 (br, 2H, PPh_2).

$^{13}C\{^1H\}$ NMR (125.7 MHz, CD_2Cl_2): δ 26.22 (d, J_{CP} = 19.7, CH_2), 28.85 (d, J_{CP} = 16.9, CH_2), 34.21 (d, J_{CP} = 30.3, CH_2-PPh_2), 125.90−127.60 (m, CH), 127.94 (d, J_{CP} = 23, C^{PPh}), 128.2−130.90 (m, CH), 131.05 (t, J_{CP} = 5.5, CH^{vinyl}), 131.30 (d, J_{CP} = 4.6, CH), 131.69 (d, J_{CP} = 21.5, C^{PPh}) 131.93 (m, C), 132.43 (d, J_{CP} = 9.2, CH^{PPh}), 133.84 (t, J_{CP} = 20, C), 134.66 (d, J_{CP} = 10.5, CH), 134.86 (d, J_{CP} = 8.6, C), 142.79 (C), 145.79 (C), 160.40 (dd, J_{CP} = 35.7, 25.2, C−Ni). $^{31}P\{^1H\}$ NMR (81.0 MHz, CD_2Cl_2): δ 2.3 (d), 28.7 (d, $^2J_{PP}$ = 318.6).

Reaction of 2b with EtC≡CPh. A solution of **2b** (60 mg, 0.085 mmol) in CD_2Cl_2 (0.7 mL) was treated with EtC≡CPh (13 μL, 1.1 equiv) to give two insertion products, [NiBr{*o*-C(Ph)═C(Et)$C_6H_4CH_2PPh_2$}($PPhBz_2$)] (**14b**) and [NiBr{*o*-C(Et)═C(Ph)$C_6H_4CH_2PPh_2$}($PPhBz_2$)] (**15b**), in a 11:1 ratio, as shown by ^{31}P NMR spectroscopy (estimated yield >80%). This sensitive mixture of complexes decomposed within 24 h at room temperature.

14b. ^1H NMR (500 MHz, CD_2Cl_2): δ 0.70 (t, J = 7.3, CH_3), 2.36 (app sept, 1H, J = 7.3, CH_2^{Et}), 2.65 (app sept, 1H, J = 7.3, CH_2^{Et}), 2.87 (dt, 1H, J = 14.8, 5.5, CH_2^{PBz}), 3.08 (t, 1H, J = 12.3, CH_2P), 3.13 (dd, 1H, J = 15, 4.5, CH_2^{PBz}), 3.66 (dd, 1H, J = 15, 6.5, CH_2^{PBz}), 3.86 (dd, 1H, J = 12, 9, CH_2P), 4.18 (dd, 1H, J = 13, 7.5, CH_2^{PBz}), 6.61 (d, 1H, J = 7.5, H^6), 6.85 (d, 2H, J = 7, H^{PPh}), 6.92 (d, 2H, J = 9, H^{Ph}), 7.00 (t, 2H, J = 8, H^{PBz}), 7.02 (t, 2H, J = 7, H^{PBz}), 7.07−7.25 (m, 11H, H^{arom}), 7.28 (d, 2H, J = 5.5, H^{PBz}), 7.31−7.50 (m, 5H, H^{arom}), 7.55 (d, 2H, J = 4, H^{PBz}), 7.59 (t, 2H, J = 7, H^{PPh_2}), 7.65 (t, 1H, J = 7, H^{4or5}), 8.16 (t, 2H, J = 8.2, H^{PPh_2}). GOESY (500 MHz, CD_2Cl_2): irradiation at δ 2.87 gave responses from δ 4.18, 6.84, 6.92, 7.00, and 7.28; irradiation at δ 3.13 gave responses from δ 6.84, 6.92, 7.00, and 7.55; irradiation at δ 8.16 gave responses from δ 3.08, 3.86, 6.92, 7.08, and 7.59. $^{13}C\{^1H\}$ NMR (125.7 MHz, CD_2Cl_2): δ 13.43 (CH_3), 25.59 (dd, J_{CP} = 18.1, 2.8, CH_2), 29.19 (dd, J_{CP} = 12.1, 1.7, CH_2), 29.27 (d, J_{CP} = 2.5, CH_2^{Et}), 33.43 (d, J_{CP} = 29.7, CH_2PPh_2), 125.99−131.50 (m, CH), 132.14 (dd, J_{CP} = 27.5, 6.6, C^{PPh}), 132.56 (d, J_{CP} = 9.9, CH^{PPh}), 132.80 (CH), 132.89 (d, J_{CP} = 2.2, CH), 132.95 (C), 133.64 (C), 134.08 (C), 134.36 (d, J_{CP} = 10.4, CH^{PPh}), 134.59 (C), 135.03 (dd, J_{CP} = 10.4, 2.2, C^{PPh}), 140.14 (br d, J_{CP} = 5, C), 140.26 (d, J_{CP} = 3.8, C), 145.62 (C), 148.75 (dd, J_{CP} = 33, 21.7, C−Ni). $^{31}P\{^1H\}$ NMR (81.0 MHz, CD_2Cl_2): δ 3.4 (d), 26.3 (d, $^2J_{PP}$ = 321.2). MALDI/TOF MS ($C_{49}H_{45}BrNiP_2$): m/z 754 (M^+ − Br).

15b. $^{31}P\{^1H\}$ NMR (81.0 MHz, CD_2Cl_2): (9.8 (d), 29.1 (d, $^2J_{PP}$ = 308.6).

Reaction of 2b with MeC≡CPPh₂. A solution of **2b** (28 mg, 0.04 mmol) in C_6D_6 (0.6 mL) was treated with 1.2 equiv. MeC≡$CPPh_2$. After 1 h at room temperature, ^{31}P NMR monitoring showed mainly broad signals of starting material and two doublets: a sharp one at δ_P 29.1 and a broad one at δ_P −106.8 (J_{PP} = 225 ± 1 Hz) due to formation of [NiBr{*o*-C(PPh_2)═C(Me)$C_6H_4CH_2PPh_2$}($PPhBz_2$)] (**18b**). After 60 h at 30 °C, no **2b** remained. The spectrum showed broad signals for **18b** and for free PBz_2Ph (δ_P −12.0) and appearance of a broad doublet at δ_P −71 ± 1 due to [NiBr{*o*-(PPh_2)(Me)C═$CC_6H_4CH_2PPh_2$}] (**19**) ($^2J_{PP}$ = 331 ± 1 Hz). Heating at 80 °C for 18 h led to a ca. 1:1 mixture of **18b** and **19**, while further heating led to decomposition.

Reaction of 2b with PhC≡CPPh₂. Reaction of **2b** (62 mg, 0.088 mmol) with 1 equiv of PhC≡$CPPh_2$ in CD_2Cl_2 (0.5 mL) gave very broad ^{31}P NMR signals. After 1 h at room temperature, the complicated spectrum showed at least three compounds: [NiBr{*o*-C(PPh_2)═C(Ph)$C_6H_4CH_2PPh_2$}($PPhBz_2$)] (**20**), having a doublet at δ_P −101.0 ($^2J_{PP}$ = 220 ± 1 Hz), [NiBr{*o*-(PPh_2)(Ph)C═$CC_6H_4CH_2PPh_2$}] (**21**), with a doublet at δ_P −68.0, and **2b**. After 48 h at 30 °C, **2b** had completely reacted to give mainly **21** and free PBz_2Ph. After filtration through SiO_2 (ether), orange crystals of **21** suitable for X-ray analysis were obtained.

21. ^1H NMR (300 MHz, CD_2Cl_2): δ 3.53 (dd, 2H, J = 9.1, 2.2, CH_2P), 6.85 (br t, 1H, J = 7, H^{Ph}), 6.95−7.25 (m, 8H, H^{arom}), 7.35−7.55 (m, 12H, H^{arom}), 7.80−7.88 (m, 4H, H^{PPh}), 7.92−8.00 (m, 4H, H^{PPh}). $^{13}C\{^1H\}$ NMR (75.4 MHz, C_6D_6): δ 32.09 (d, J_{CP} = 24.7, CH_2PPh_2), 126.80−134.00 (m, CH + C), 135.29 (m, C), 136.67 (C), 138.15 (d, J_{CP} = 14.2, C), 142.30 (d, J_{CP} = 41.7, C), 148.23 (dd, J_{CP} = 44, 5, C). $^{31}P\{^1H\}$ NMR (81.0 MHz, CD_2Cl_2): δ −67.7 (d), 32.0 (d, $^2J_{PP}$ = 308.7). EI-MS ($C_{39}H_{31}BrNiP_2$): m/z 619 (6, M^+ − Br), 439 (17), 307 (33), 286 (100), 261 (28).

X-ray Crystallography. Crystal data and details of data collection, data processing, structure analysis, and structure refinement are given in Table 8. All crystals were mounted on a quartz fiber, the data for **4b**·0.5C_6H_6 being recorded at −80 °C, those for **6b** and **10b** at −73 °C, and those for the other two (**17**·CH_2Cl_2 and **21**) at 23 °C. The structures of **4b**·0.5C_6H_6, **6b**, and **21** were solved by direct methods (SIR92)[48] and those of **17**·CH_2Cl_2 and **10b** by Patterson methods (PATTY);[49] all were expanded with use of Fourier techniques (DIRDIF94).[50] The diffractions of **6b** and **10b** were measured by a 95 mm CCD camera, and the intensities of the reflections were processed by use of the computer programs Denzo and Scalepak.[51] Besides the molecular species **4b**, the crystallographic asymmetric unit also contained 0.5 molecule of benzene. The non-hydrogen atoms were refined anisotropically by full-matrix least squares. Hydrogen atoms were included at geometrically determined positions (C−H = 0.95 Å) and periodically recalculated, but they were not refined. The maximum and minimum peaks in the final difference Fourier map were 0.95 and −0.79 e/Å^3, respectively.

The crystal of **6b** was of very good quality, and all non-hydrogen atoms were refined anisotropically by full-matrix least squares, whereas the hydrogen atoms were refined isotropically. The maximum and minimum peaks in the final difference Fourier map were 0.36 and −0.72 e/Å^3, respectively.

The crystal of **10b** was of poor quality and diffracted weakly. However, a highly restrained refinement yielded a clearly defined molecular structure. The geometries of the phenyl rings such as bond lengths and angles and planarity were imposed. All non-hydrogen atoms were refined anisotropically by full-matrix least squares. Hydrogen atoms were included at calculated positions (C−H = 1.00 Å) and left riding with their carbon of attachment. The maximum and minimum peaks in the final difference Fourier map were 1.46 and −0.95 e/Å^3, respectively.

In the crystal structure of **17**·CH_2Cl_2, the molecular species was a dimer containing a 2-fold rotation axis coincident with a crystallographic 2-fold axis. A molecule of CH_2Cl_2 was also

(48) Altomare, A.; Cascarano, M.; Giacovazzo, C.; Guagliardi, A.; Burla, M. C.; Polidori, G.; Camalli, M. *J. Appl. Crystallogr.* **1994**, *27*, 435.

(49) Beurskens, P. T.; Admiraal, G.; Beurskens, G.; Bosman, W. P.; Garcia-Granda, S.; Gould, R. O.; Smits, J. M. M.; Smykalla, C. The PATTY and DIRDIF Program System; Technical Report of the Crystallographic Laboratory; University of Nijmegen, Nijmegen, The Netherlands, 1992.

(50) Beurskens, P. T.; Admiraal, G.; Beurskens, G.; Bosman, W. P.; de Gelder, R.; Israel, R.; Smits, J. M. M. The DIRDIF-94 Program System; Technical Report of the Crystallographic Laboratory; University of Nijmegen, Nijmegen, The Netherlands, 1994.

(51) Otwinowski, Z.; Minor, W. In *Methods in Enzymology*; Carter, C. W., Jr.; Sweet, R. M., Ed.; Academic Press: New York, 1997; Vol. 276, p 307.

Table 8. Crystal and Structure Refinement Data for Compounds 4b, 6b, 10b, 17, and 21

	4b	6b	10b	17	21
			(a) Crystal Data		
chem formula	$C_{47}H_{44}BrNiO_2P_2 \cdot 0.5C_6H_6$	$C_{43}H_{39}BrNiO_2P_2$	$C_{45}H_{40}BrF_3NiO_2P_2$	$(C_{35}H_{29}BrNiO_2P_2)_2 \cdot CH_2Cl_2$	$C_{39}H_{31}BrNiP_2$
fw	841.41	788.35	870.37	1449.26	700.23
cryst syst	triclinic	monoclinic	monoclinic	monoclinic	monoclinic
unit cell dimens					
a (Å)	9.776(3)	17.6495(2)	27.914(2)	18.610(4)	10.870(3)
b (Å)	14.482(4)	10.56920(10)	15.4458(10)	15.700(2)	22.707(4)
c (Å)	15.326(4)	20.3919(2)	18.9929(12)	22.175(3)	13.162(3)
α (deg)	76.36(2)				
β (deg)	75.75(2)	99.0906(5)	99.506(4)	105.55(1)	96.32(2)
γ (deg)	77.03(2)				
V (Å^3)	2012(1)	3756.15(7)	8076.4(8)	6242(2)	3229(1)
space group	$P\bar{1}$ (No. 2)	$P2_1/a$ (No. 14)	$C2/c$ (No. 15)	$C2/c$ (No. 15)	$P2_1/n$ (No. 14)
D_c (g cm^{-3})	1.389	1.394	1.432	1.542	1.440
Z	2	4	8	4	4
F(000)	870	1624	3567	2952	1432
color, habit	yellow, block	orange, prism	orange-red, block	orange, needle	orange, wedge
cryst dimens (mm)	0.34 × 0.19 × 0.12	0.15 × 0.18 × 0.08	0.19 × 0.20 × 0.17	0.30 × 0.03 × 0.01	0.30 × 0.15 × 0.10
μ(cm^{-1})	29.03 (Cu Kα)	1.70 (Mo Kα)	1.60 (Mo Kα)	44.08 (Cu Kα)	34.67 (Cu Kα)
			(b) Data Collection and Processing		
diffractometer	Rigaku AFC6R	Nonius KappaCCD	Nonius KappaCCD	Rigaku AFC6R	Rigaku AFC6R
X-radiation	Cu Kα (graphite monochrom)	Mo Kα (graphite monochrom)	Mo Kα (graphite monochrom)	Cu Kα (graphite monochrom)	Cu Kα (graphite monochrom)
$2\theta_{max}$ (deg)	120.0	54.96	46.9	120.0	120.2
data collected (*h*,*k*,*l*)	(−10,−15,0) to (10,16,17)	(−22,−13,−26) to (22,13,26)	(−31,−17,−21) to (31,17,19)	(0,0,−24) to (20,17,24)	(−12,0,0) (12,25,14)
no. of rflns					
total	6219	83 662	17 820	5022	5193
unique (R_{int} (%))	5960 (5.1)	8598 (5.0)	5779 (8.5)	4813 (21.0 for 0*kl*)	4801 (12.1)
obsd	5330 ($I > 2\sigma(I)$)	7062 ($I > 3\sigma(I)$)	4643 ($I > 3\sigma(I)$)	1706 ($I > 3\sigma(I)$)	2527 ($I > 2\sigma(I)$)
abs cor (transmissn factors)	analytical (0.5322−0.7155)	integration (0.774−0.877)	integration (0.724−0.814)	azimuthal scans (0.81−0.96)	analytical (0.60−0.78)
decay (%)	none	none	none	1.8	1.59
			(c) Structure Analysis and Refinement		
structure soln	direct methods (SIR92)	direct methods (SIR92)	Patterson methods (PATTY)	Patterson methods (PATTY)	direct methods (SIR92)
refinement			full-matrix least squares		
no. of params	478	481	488	166	388
R(obsd data) (%)	4.5	4.3	12.4	9.4	4.9
R_w(obsd data) (%)	6.2	3.7	9.8	11.8	5.4

present but was 4-fold disordered. The crystal data, obtained from a very thin needle, were of limited quality, and only 1706 out of 4813 independent measured reflections were considered reliable. As a consequence, the comprehensive constrained least-squares refinement software RAELS96[52] was used, and the use of constraints[53−55] enabled 166 variables to adequately describe the refinement of the 47 non-H atom sites. The Ni and Br atoms were refined as anisotropic atoms, but refinable rigid-body thermal parametrizations were used for all the other atoms.[53] Hydrogen atoms were included at calculated positions (C−H = 0.96 Å) after each refinement cycle. The maximum and minimum peaks in the final difference Fourier map were 1.39 and −0.97 e/Å^3, respectively, located close to the Ni or Br atoms.

The non-hydrogen atoms of complex **21** were refined anisotropically by full-matrix least squares. Hydrogen atoms were included at geometrically determined positions (C−H = 0.95 Å) and periodically recalculated, but they were not refined. The maximum and minimum peaks in the final difference Fourier map were 0.48 and −0.38 e/Å^3, respectively.

The calculations were performed with use of the crystallographic software packages teXsan,[56] RAELS96,[52] maXus,[57] and CRYSTALS.[58]

The neutral atom scattering factors were taken from ref 59 for structure **17** and from ref 60 for all other structures. $\Delta f'$ and $\Delta f''$ values and mass attenuation coefficients were taken from ref 55 for **17** and from ref 61 for all other structures.

Computational Details. Density functional calculations used the Amsterdam Density Functional program ADF1999.[62] All atoms were described by a double-ζ plus polarization STO basis set with the frozen-core approximation being employed for the 1s electrons of C, N, O, and F atoms and up to the 2p electrons of Si and P. Geometry optimizations included the gradient corrections of Becke[63] and Perdew[64] as well as the

(52) Rae, A. D. RAELS96: A Comprehensive Constrained Least-Square Refinement Program; Australian National University, Canberra, ACT, Australia, 1996.
(53) Rae, A. D. *Acta Crystallogr.* **1975**, *A31*, 560, 570.
(54) Rae, A. D. *Acta Crystallogr.* **1984**, *A40* (Supplement), C428.
(55) Haller, K. J.; Rae, A. D.; Heerdegen, A. P.; Hockless, D. C. R.; Welberry, T. R. *Acta Crystallogr.* **1995**, *B51*, 187.
(56) TEXSAN: Single-Crystal Structure Analysis Software, Version 1.8; Molecular Structure Corp., 3200 Research Forest Drive, The Woodlands, TX 77381, 1997.
(57) Mackay, S.; Gilmore, C. J.; Edwards, C.; Stewart, N.; Shankland, K. maXus Computer Program for the Solution and Refinement of Crystal Structures; Nonius, MacScience, and The University of Glasgow, 1999.
(58) Watkin, D. J.; Prout, C. K.; Carruthers, J. R.; Betteridge, P. W. CRYSTALS Issue 10; Chemical Crystallography Laboratory, Oxford, U.K., 1996.
(59) *International Tables for Crystallography*; Wilson, A. J. C., Ed.; Kluwer Academic: Dordrecht, The Netherlands, 1995; Vol. C.
(60) Cromer, D. T.; Waber, J. T. *International Tables for X-ray Crystallography*; Kynoch Press: Birmingham, England, 1974; Vol. IV.
(61) *International Tables for Crystallography*; Wilson, A. J. C., Ed.; Kluwer Academic: Dordrecht, The Netherlands, 1992; Vol. C.
(62) (a) Baerends, E. J.; Ellis, D. E.; Ros, P. *Chem. Phys.* **1973**, *2*, 41. (b) te Velde, G.; Baerends, E. J. *J. Comput. Phys.* **1992**, *99*, 84. (c) Fonseca Guerra, C.; Snijders, J. G.; te Velde, G.; Baerends, E. J. *Theor. Chem. Acc.* **1998**, *99*, 391.
(63) Becke, A. D. *Phys. Rev. A* **1988**, *38*, 3098.
(64) Perdew, J. P. *Phys. Rev. B* **1986**, *33*, 8822.

quasi-relativistic corrections of Snijders and co-workers.[65] The optimization procedure developed by Versluis and Ziegler was employed.[66] Alkyne structures were optimized in C_{3v} or C_s symmetry as appropriate.

(65) (a) Snijders, J. G.; Baerends, E. J.; Ros, P. *Mol. Phys.* **1979**, *38*, 1909. (b) Ziegler, T.; Tschinke, V.; Baerends, E. J.; Snijders, J. G.; Ravenek, W. *J. Phys. Chem.* **1989**, *93*, 3050. (c) van Lenthe, E.; Baerends, E. J.; Snijders, J. G. *J. Chem. Phys.* **1993**, *99*, 4597.

(66) (a) Versluis, L.; Ziegler, T. *J. Chem. Phys.* **1988**, *88*, 322. (b) Fan, L.; Ziegler, T. *J. Am. Chem. Soc.* **1992**, *114*, 10890.

Acknowledgment. E.W. is grateful to the Australian Research Council for the award of a QEII Research Fellowship. S.A.M. thanks the EPSRC for funding.

Supporting Information Available: Tables giving full crystallographic data for **4b**·0.5C_6H_6, **6b**, **10b**, **17**·CH_2Cl_2, and **21**. This material is available free of charge via the Internet at http://pubs.acs.org.

OM0101083